공학박사 학위논문

Dispersibility and mechanical properties of polyetheretherketone/ hydroxyapatite/carbon fiber composites prepared by non-melt blending method

비용융 혼합 방식으로 제조한 수산화인회석과 탄소섬유를 함유하는 폴리에테르에테르케톤 복합재의 분산성 및 기계적 물성

2021년 08월

서울대학교 대학원

화학생물공학부

전 인 성

Dispersibility and mechanical properties of polyetheretherketone/hydroxyapatite/carbon fiber composites prepared by non-melt blending method

비용융 혼합 방식으로 제조한 수산화인회석과 탄소섬유를 함유하는 폴리에테르에테르케톤 복합재의 분산성 및 기계적 물성

지도교수 조 재 영

이 논문을 공학박사 학위논문으로 제출함
2021년 07월

서울대학교 대학원
화학생물공학부
전 인 성

전인성의 공학박사 학위논문을 인준함
2021년 06월

위 원 장 _____

부위원장 _____

위 원 _____

위 원 _____

위 원 _____

Abstract

Polyetheretherketone (PEEK), a member of the polyaryletherketone family, is a semi-crystalline thermoplastic polymer with combinations of ketone and ether functional groups. Due to its unique chemical structure, PEEK confers outstanding chemical resistance, mechanical properties, and biocompatibility. Thereby, PEEK has been a primary candidate to replace metallic implant components in the field of orthopedic surgery. However, the mechanical strength and the bioactivity of PEEK should be improved to be used as spinal implant component. To improve the mechanical strength and bioactivity of PEEK, PEEK is generally reinforced with carbon fiber (CF) and hydroxyapatite (HA) fillers. However, PEEK/HA/CF composites manufactured by the melt-extrusion process, commonly used in industry, are significantly inferior in processability due to the aggregation of nano-sized HA filler and de-bonding between the PEEK matrix and the fillers. Thus, other effective blending methods should be applied before the melt-extrusion process. In this study, two different fabrication methods (suspension blending and mechanofusion) were carried out to investigate the improvement in mechanical properties of PEEK/HA/CF composite.

First, PEEK/HA/CF composite was prepared by suspension blending using surface modified HA and CF fillers. The surface modification was performed primarily with a silane coupling agent and secondly with succinic anhydride.

The PEEK/HA/CF composite prepared in this way showed excellent improvement in both flexural and compressive strengths compared to the composite reinforced with unmodified fillers. The results of SEM and XRM analysis confirmed that both interfacial adhesion between the PEEK matrix and the fillers and dispersibility of HA were improved by surface modification on HA and CF fillers. Besides, HA nanofiber (HANF) was also used as reinforcement for PEEK composite. Due to its high elastic modulus and high aspect ratio, the PEEK/HANF/CF composite exhibited the highest mechanical strength, which was further enhanced after surface modification of fillers. These improvements were due to the enhanced dispersibility and interfacial adhesion of HANF and CF in the PEEK matrix, confirmed by SEM and XRM.

Second, the PEEK/HA/CF composite was prepared by mechanofusion process, one of non-melt blending methods that can be performed in dry condition. The mechanofusion process is better method than the suspension blending method because it does not use any solvents. By mechanofusion process, the result of SEM confirmed that HA nanoparticles were uniformly coated on the surface of PEEK particles and micro-sized CF filler. This phenomenon could impede the formation of HA aggregates and helped the dispersion of HA filler during the injection molding process for PEEK/HA/CF composite. The PEEK/HA/CF composite prepared by mechanofusion method showed higher flexural and compressive strengths than the composite prepared by suspension blending method. The XRM analysis confirmed the enhanced dispersion of HA filler. Moreover, higher mechanical strength can

be expected if the PEEK/HA/CF composite are prepared by the mechanofusion method using surface modified HA and CF.

Finally, instead of using commercial PEEK, synthesized P(E2-E4)K polymer was used for the composite. In addition to CF, graphene oxide (GO), which has high surface area and various surface functional groups, had been introduced into P(E2-E4)K composite. GO was expected to increase the flexural strength with a small content compared to CF. But, the flexural strength was improved a little bit due to the aggregation of GO nanosheets. However, it was confirmed that the flexural strength of P(E2-E4)K/GO/CF composite is within the range of cortical bone if 30 wt% of CF was used.

Key words : polyetheretherketone composite, mechanical properties, mechanofusion, suspension blending, filler dispersion, hydroxyapatite nanofiber

Student number : 2016-21051.

Table of Contents

Chapter 3
Mechanical Properties of Polyetheretherketone/hydroxyapatite/carbon fiber Composite prepared by Mechanofusion Process

Chapter 4
Mechanical Strength of Polyetheretherketone Copolymer Composite Reinforced with Graphene Oxide and Carbon Fiber

List of Tables

List of Figures

Chapter 1

Introduction

1.1. Polyetheretherketone composite for spinal implants

Polyetheretherketone (PEEK), one of the high-performance plastics, is a semi-crystalline thermoplastic polymer that was first developed in 1978 [1]. Since then, PEEK was commercialized for various industrial fields such as aerospace, automotive, electronic, and medical sectors. PEEK is a member of the polyaryletherketone family consisting of an aromatic molecular backbone with combinations of ketone and ether functional groups. The unique chemical structure of PEEK confers outstanding chemical resistance, mechanical properties, thermal stability, wear-resistance, and biocompatibility [2]. Based on the unique features of PEEK described above, PEEK has been primary candidate to replace metallic implant components by the late 1990s [3].

Even though the metal components provide excellent mechanical strength, friction resistance, and biocompatibility, their disadvantages like stress shielding effect, image distortion, and release of ions have hindered their medical applications [4]. For example, the elastic modulus of metals ($\geq$110 GPa) is much higher than that of human cortical bone (~14 GPa), which can result in stress shielding and bone resorption on the bone around the implant [5]. As a substitution for metals, carbon fiber reinforced polyetheretherketone (CFR-PEEK) has been widely used in orthopedic and spinal implants because the mechanical properties were close to those of human cortical bone. However, the lack of surface functional groups on CF usually results in weak interfacial adhesion with PEEK matrix in the composites. Moreover, the

hydrophobicity of carbon fibers in CFR-PEEK impedes in vivo osteointegration and can weaken the bioactivities such as cell attachment, spreading, and proliferation [6].

While PEEK is a biocompatible polymer, it does not osseointegrate in vivo and does not provoke interactions with bone tissue [7]. In order to improve the bioactivity of PEEK composite, hydroxyapatite (HA), one of calcium phosphate ceramics, is commonly used as filler material for PEEK composite. Due to its similarity to human bone mineral, HA induces the bone to grow and restores the defect. Several studies reported that HA reinforced PEEK composite exhibited better cell proliferation, osteogenic differentiation, and osteoblast growth than the neat PEEK [8-10]. However, one of the common issues encountered by many researchers from using HA nanoparticles is the agglomeration of nano-sized HA, which becomes severe as the content of HA increases due to high specific surface area and ion-ion interaction between Ca^{2+} and OH^- groups on the surface of HA [11-15]. This aggregation can cause early fracture of PEEK composite and consequently decrease the mechanical properties. In addition to bioactivity, HA can be used as a nanofiber form, HA nanofiber (HANF), to improve the mechanical properties of PEEK composites. Based on the previous studies, HANF reinforced composite exhibits improved mechanical properties due to the high surface area-to volume ratio and the bridging effect of fiber [16-18].

Recent studies also reported that the mechanical properties and bioactivity were simultaneously improved in PEEK composites reinforced with HA and CF fillers together [19,20]. Nevertheless, the poor processability of

PEEK/HA/CF composite due to excessive filler use, aggregation of nano-sized HA filler, and de-bonding between the PEEK matrix and the fillers were the major problems to be solved. In other words, the content of CF in the composite should be adjusted at the level of mechanical properties similar to that of cortical bones, and the content of HA should be adjusted in a way that mechanical properties are not severely deteriorated due to aggregation.

1.2. Surface modification of fillers

The surface modification of fillers using silane coupling agents is one of the methods for improving both dispersibility of nanoparticles and interfacial adhesion between fillers and PEEK matrix. The silane coupling agent works as ‘bridge linkage’ between the inorganic filler and the polymer matrix. The most popular modification agent for fillers with hydroxyl functional groups is 3-aminopropyltriethoxysilane (APTES), which has alkoxysilyl groups on one side and an amine group on the other. In general, the alkoxysilyl groups of the silane coupling agent react with water to form silanol groups by hydrolysis. These silanol groups can either form siloxane linkages each other or form covalent bonds with the hydroxyl groups of inorganic filler by condensation reaction. Then, the inorganic filler with amine end group can react with the functional groups of polymer. This amine end group, which has hydrophobic and positively charged properties, may cause a toxic reaction with negatively charged cell membranes by electrostatic interaction in vivo. Therefore, it is necessary to change the amine end group to carboxyl end group using succinic anhydride, which can induce the growth of osteoblasts due to hydrophilic and negatively charged properties. The surface modification of HA not only can lower its surface area but also can weaken the ion-ion interaction between HA nanoparticles by covering the Ca^{2+} ions on the surface with the carboxyl end groups. Thus, the dispersion of HA could be improved. The formation of carboxyl end groups on the surface of CF improved the interfacial adhesion with PEEK matrix by hydrogen bonding with ketone functional groups of

PEEK. Furthermore, the silane coupling treatment is known for not only improving the interfacial bonding and wettability of modified filler, but also preventing filler from external damages during the manufacture processing [7]. Some recent researches report that the surface modification of HA filler with silane coupling agent enhanced the interface bonding and dispersion of HA particles in PEEK/HA composites and increased the mechanical strength [21-23]. Surface modification on CF surface also shows improved interfacial adhesion with polymer matrix [24,25].

1.3. Non-melt blending methods

A common method for PEEK composite fabrication in industrial fields is the melt processing method using an extruder equipped with high temperature heater. In melt blending, nano-sized HA filler is introduced and mixed with PEEK polymer in molten state. Regardless of several advantages of the melt extrusion process like low-cost, solvent-free, and strong mechanical force for mixing, such method sometimes cannot provide sufficient dispersibility for nano-sized fillers in high contents due to increased viscosity. Moreover, it is difficult to have an extrusion machine that satisfies the conditions of PEEK composites that require temperature above 360 ℃ in a lab scale. Thus, an effective blending method that can improve dispersibility of nano-sized fillers, preferably at room temperature, is required.

One of the non-melt blending methods that can enhance the dispersion of nano-fillers in the lab-scale is ultrasonication followed by suspension blending in ethanol. The sonication treatment is a form of vibration that generates cavitation or bubbles and provides high intensity of ultrasound energy to the filler [26]. By applying sonication and suspension blending in ethanol, the aggregates of nanoparticles can be disintegrated and uniformly dispersed in the ethanol suspensions without significant deformation or defects [27]. Thus, the wet mixing process described above can be applied to the preparation of PEEK/HA/CF composite in order to enhance the dispersibility of HA filler.

Even though the wet mixing process is widely used in lab scale due to

simplicity, it is not convenient in industrial aspects due to low processability, high production cost, and environmental pollution by the solvents used. As an alternative to the suspension blending method, mechanofusion, one of dry powder coating system, is an adequate approach to enhance both dispersibility of aggregated filler and compatibility between polymer matrix and filler by high shear and compressive forces on the powder mixture [28,29]. By applying mechanofusion process, HA nanoparticles are expected to be dry coated onto the surface of micro-sized CF and PEEK powder. Moreover, HA aggregates are expected to be broken down to smaller size by mechanical forces produced by rotating blades in the chamber. Thereby, the mechanical properties of PEEK/HA/CF composite can be improved due to enhanced dispersibility of HA nanoparticles.

1.4. Motivation

Based on the understanding of shortcomings of the melt extrusion method for manufacturing PEEK/HA/CF composite in the laboratory scale, other effective blending methods are needed in order to improve the mechanical properties of PEEK/HA/CF composite. The main drawbacks in the processability of PEEK/HA/CF composite are not only the poor interfacial adhesion between the fillers and the PEEK matrix but also the aggregation of HA nanoparticles. Prior to the melt extrusion or injection molding process, such limitations can be overcome by applying surface modification on fillers and using non-melt blending methods such as suspension blending and mechanofusion process. The surface modification of fillers using silane coupling agent is expected to enhance not only the dispersion of nano filler but also the interfacial adhesion between the fillers and the PEEK matrix. Moreover, the suspension blending with ultrasonication, which can be done easily in lab scale, is a wet-process blending that is expected to provide enhanced dispersibility of nano-sized HA filler by the ultrasound energy and the mechanical collision in ethanol suspensions. However, the main issue of the suspension blending method is the solvents used during the process. Thus, the mechanofusion process, which does not use any solvent, is expected to be another adequate method for manufacturing PEEK/HA/CF composite. Thereby, in this study, the effect of surface modified filler and mechanofusion process on the mechanical properties of PEEK/HA/CF composite is investigated.

1.5. References

[1] L. Eschbach, *Injury*, **2000**, *31*, 22.

[2] M. McHugh, V. J. Krukonis, Encyclopedia of Polymer Science and Engineering, **1989**, John Wiley and Sons, Inc. New York.

[3] S. M. Kurtz, J. N. Devine, *Biomaterials*, **2007**, *28*, 4845.

[4] M. I. Z. Ridzwan, S. Shuib, A. Y. Hassan, A. A. Shokri, M. N. M. Ibrahim, M. N. Mohammad Ibrahim, *J. Med. Sci.*, **2007**, *7*, 460.

[5] J. Y. Rho, R. B. Ashman, C. H. Turner, *J Biomech.* **1993**, *26*, 111.

[6] C. S. Li, C. Vannabouathong, S. Sprague, M. Bhandari, *Clin. Med. Insights Arthr. Musculoskelet. Disord.* **2015**, *8*, 33.

[7] T. Wang, Y. Jiao, Z. Mi, C. Wang, D. Wang, X. Zhao, H. Zhou, C. Chen, *Chemistry Select*, **2020**, *5*, 5507.

[8] Y. Zhang, L. Hao, M. M. Savalani, R. A. Harris, L. di Silvio, K. E. Tanner, *J. Biomed. Mater. Res. A*, **2009**, *91*, 1018.

[9] D. Almasi, S. Izman, M. Sadeghi, N. Iqbal, F. Roozbahani, G. Krishnamurithy, T. Kamarul, M. R. Abdul Kadir, *Int. J. Biomater*., **2015**, *2015*, 5.

[10] L.L. Hench, *J. Am. Ceram. Soc*., **1991**, *74*, 1487.

[11] M. S. AbuBakar, P. Cheang, K. A. Khor, *Compos. Sci. Technol*. **2003**, *63*, 421.

[12] J. P. Fan, C. P. Tsui, C. Y. Tang, *Mater. Sci. Eng. A*, **2004**, *382*, 341.

[13] S. M. Tang, P. Cheang, M. S. AbuBakar, K. A. Khor, K. Liao, *Int. J. Fatigue*, **2004**, *26*, 49.

[14] P. Cheang, K. A. Khor, *Mater. Sci. Eng. A*, **2003**, *345*, 47.

[15] R. K. Roeder, M. M. Sproul, C. H. Turner, *J. Biomed. Mater. Res.*, **2003**, *67A*, 801.

[16] K. G. Dassios, *Adv. Compos. Lett*., **2007**, *16*, 17.

[17] L. Chen, Q. Yu, Y. Wang, H. Li, *Dent. Mater*., **2011**, *27*, 1187.

[18] H. -S. Ko, S. Lee, J. Y. Jho, *Nanomaterials*, **2021**, *11*, 213.

[19] Y. Deng, P. Zhou, X. Liu, L. Wang, X. Xiong, Z. Tang, J. Wei, S. Wei, *Colloids Surf. B*, **2015**, *136*, 64.

[20] X. Feng, G. Sui, R. Yang, *Chin. J. Mater. Res*. **2008**, *22*, 18.

[21] R. Ma, Q.. Li, L. Wang, X. Zhang, L. Fang, Z. Luo, B. Xue, L. Ma, *Mater. Sci. Eng. C*., **2017**, *73*, 429.

[22] A. M. P. Dupraz, J. R. de Wijin, S. A. T. v.d. Meer, K. de Groot, *J. Biomed. Mater. Res*. **1996**, *30*, 231.

[23] P. Roy, R. R. N. Sailaja, *J. Mech. Behav. Biomed*., **2015**, *49*, 1.

[24] H. Yuan, C. Wang, S. Zhang, X. Lin, *Appl. Surf. Sci*., **2012**, *259*, 288.

[25] L. Hao, Y. Hu, Y. Zhang, W. Wei, X. Hou, Y. Guo, X. Hu, D. Jiang, *RSC Adv.*, **2018**, *8*, 27304.

[26] I. Kaur, L. J. Ellis, I. Romer, R. Tantra, M. Carriere, S. Allard, M. Mayne-L'Hermite, C. Minelli, W. Unger, A. Potthoff, S. Rades, E. Valsami-Jones, *J. Vis. Exp.*, **2017**, *130*, e56074.

[27] T. Peng, I. Chang, *Powder Technol*., **2015**, *284*, 32.

[28] D. Wei, R. Dave, R. Pfeffer, *J. Nanopart. Res*., **2002**, *4*, 21.

[29] S. B. Park, M. S. Lee, M. Park, *Carbon Let*., **2014**, *15*, 117.

Chapter 2

Mechanical Properties of Polyetheretherketone/hydroxyapatite nanofiber/carbon fiber Composites with Surface Modified Fillers

2.1. Introduction

Metals, such as titanium (Ti) alloy, stainless steel, tantalum (Ta), and cobalt chromium (Co-Cr) alloy, have been extensively used for spinal implants because of their excellent mechanical strength, friction resistance, and biocompatibility. However, some disadvantages like stress shielding effect, image distortion, and release of ions have hindered their other medical applications [1,2]. For example, mismatch in strength and elastic modulus ($\geq$ 110 GPa) of metals with those of human cortical bone (~14 GPa) can cause stress shielding and bone resorption on the bone around the implant [3]. As an alternative material that can overcome the disadvantages of metal implants, carbon fiber reinforced polyetheretherketone (CFR-PEEK) has been widely used in orthopedic and spinal implants due to its favorable mechanical strength, chemical resistance, biocompatibility, and MRI compatibility [4,5]. Nevertheless, the hydrophobicity of carbon fibers in CFR-PEEK impedes in vivo osteointegration and can weaken the bioactivities such as cell attachment, spreading, and proliferation [6].

In order to improve bioactivity of CFR-PEEK composite, some recent studies incorporated hydroxyapatite (HA) filler, a constituent of living bone, to make PEEK/HA/CF ternary composites [7,8,9]. HA is one of bioactive fillers that have been widely used in orthopedic implants because of its osteoconductive abilities, improving bone integration and regeneration [10]. Yet, HA easily forms aggregates in HA reinforced PEEK composites due to high surface area. Aggregation of HA particles and debonding between HA

and PEEK matrix are the major issues that has to be improved because they can result in severe reduction in mechanical properties of PEEK/HA/CF ternary composites.

The general approach to improve the dispersion of HA and the interface bonding between HA and PEEK has been the surface modification of HA filler. Some recent researches report that the surface modification of HA filler with silane coupling agent enhanced the interface bonding and dispersion of HA particles in PEEK/HA composites and increased the mechanical strength [11,12]. Rashidi et al. [13] also reported that silane coupled PEEK/HA composites showed improvements in biomechanical properties without cytotoxicity in vitro. The silane coupling agent can work as ‘bridge linkage’ between HA and polymer matrix for improving the interfacial bonding strength. Moreover, it can reduce the surface energy of HA filler and improve dispersion of particles in the PEEK/HA/CF composite. Esmaeilzadeh et al. [14] showed that the cell adhesion and proliferation of composites modified with (3-aminopropyl)triethoxysilane (APTES) coupling agent exhibited improved in vitro cell growth and attachment. On the other hand, some researchers reported that amine-functionalized HA with APTES showed a reduction in bioactivity and slight toxicity from in vivo tests [15,16]. Thereby, amine-functionalized HA should be used after post-functionalization with succinic anhydride, which introduces negatively charged carboxyl end group to HA.

Another way for improving both mechanical properties and bioactivity of CFR-PEEK composites is the addition of HA nanofiber (HANF). It has been

shown that the mechanical properties of polymers can be improved by using nano-scale fibrous filler due to the high surface area-to volume ratio [17,18]. For example, Chen et al. [19] reported that the dental composites reinforced with HANF substantially improved the biaxial flexural strength due to the good dispersion of HANF. Ko et al. [20] compared PLA composites reinforced by rod-like HA and HANF, and the results showed that the tensile and flexural strength of PLA composite increased from 61 to 77 MPa and from 81 to 107 MPa, respectively, due to the increased aspect ratio and the bridging effect of fiber. The results also showed that the mechanical strength of PLA/HANF composite can be further improved by using HANF with higher aspect ratio. However, the reliability of the results was insufficient since there were only two comparison groups. To the best of our knowledge, there is no report on the mechanical properties of PEEK/HANF/CF ternary composite. Thus, in this study, we prepared HA nanofiber and performed surface modification on HA, HANF, and CF fillers to improve the dispersion of fillers in PEEK composites. We evaluated the flexural properties and compressive strength of both PEEK/HA/CF and PEEK/HANF/CF composites with the addition of surface modified HA, HANF, and CF fillers.

2.2. Materials and Methods

Materials

The PEEK powder obtained from Victrex (450PF, South Carolina, USA) was used as-received. Hydroxyapatite powder with average particle size of 20 nm in width and 150 nm in length was purchased from Nanjing Emperor Nano Material Co. Ltd. (Nano HAP04, Nanjing, China). Carbon fiber powder with a measured density of 1.81 g/cm^3 was purchased from Zoltek (PX 35, Missouri, USA). The average length and diameter of CF were 150 and 7.2 μm, respectively. In this study, milled carbon fiber was used instead of short carbon fiber because the bundles of short carbon fiber could not be untangled with suspension blending method due to weak mechanical force compared to the melt-extrusion method. Calcium nitrate tetrahydrate ($Ca(NO_3)_2 \cdot 4H_2O$), ammonium phosphate dibasic ($(NH_4)_2HPO_4$), urea, nitric acid (HNO_3, 70%), dimethyl sulfoxide (DSMO), succinic anhydride (SAH), and ethanol were purchased from Daejung Chemicals (Gyeonggi-do, Korea). APTES was purchased from IruChem (IRUSIL A1100, Seoul, Korea). All the other chemicals were purchased from Sigma-Aldrich Corporation.

Preparation of HANF

HANF used in this study was synthesized using the homogeneous co-precipitation method as described in detail elsewhere [20,21]. A schematic of HANF synthesis is shown in **Figure 2.1**. The aqueous solutions of 0.16 M $Ca(NO_3)_2 \cdot 4H_2O$, 0.1 M $(NH_4)_2HPO_4$, and 0.5 M urea were separately

prepared in 300 mL of distilled water. 0.1 M $(NH_4)_2HPO_4$ solution was added dropwise to 0.16 M $Ca(NO_3)_2 \cdot 4H_2O$ aqueous solution, and then 0.5 M HNO_3 was added to the mixture until the desired pH was reached. After adding the aqueous solution of 0.5 M urea, the mixture was sealed and placed in an oven at a temperature of 95 ℃ for 80 hr. The mixture was filtered and washed with distilled water, followed by an ethanol washing to remove the residual ions and water. Then, the produced HANF powders were dried at 90 ℃ for 24 hr.

Surface modification of HA, HANF, and CF

The surfaces of HA, HANF, and CF fillers were modified in two steps: silanization with APTES and carboxylation with SAH. In a typical procedure, 10.0 g of filler in ethanol was sonicated for 1 hr. Then, 100 ml of deionized water and 2.5 ml of APTES were added and stirred at 60 ℃ for 12 hr. The precipitate was filtered and added to 200 ml of DMSO containing excess amount of SAH, followed by stirring for 24 hr. The product was then filtered, washed with ethanol 4 times, and vacuum-dried at 80 ℃ for 24 hr. The surface modified HA, HANF, and CF fillers are named as m-HA, m-HANF, and m-CF, respectively.

Preparation of composite powders

PEEK/HA/CF and PEEK/m-HA/m-CF composites were prepared according to the composition provided in **Table 2.1** using suspension blending method in ethanol. A schematic of suspension blending method to prepare PEEK composite is shown in **Figure 2.2**. The PEEK powder and fillers were

separately dispersed in ethanol, followed by ultrasonication for 1.5 hr. Then, each dispersed solution was mixed with another and stirred for 24 hr. The composite suspension was filtered and vacuum-dried at 80 ℃ for 24 hr. PEEK/HANF/CF and PEEK/m-HANF/m-CF composites were prepared by same procedure according to the composition provided in **Table 2.2**. The composites reinforced by m-HA, m-HANF, and m-CF were named as same designation with 'm-' prefix (e.g. m-H1, m-HF1, m-H1C1, and m-HF1C1).

Characterization

The size of synthesized HANF was measured from scanning electron microscopy (SEM, SUPRA 55VP, ZEISS) images by counting at least 100 individual fibers. The X-ray diffraction (XRD) of HANF was characterized using Cu-Kα radiation source (1.54 Å) in a Rigaku SmartLab XRD instrument.

To determine the chemical changes after surface modification, the surface of each fillers was analyzed by X-ray photoelectron spectroscopy (XPS, K-alpha^{+}, ThermoFisher Scientific) with Al Kα excitation radiation. The XPS measurements were performed over the high sensitivity spectrum of N1s and C1s with pass energy of 40 eV and the wide scanning energy range from 0 to 1350 eV with pass energy of 200 eV. The spectral analysis was performed by Fourier transform-infrared (FTIR, TENSOR27, Bruker) spectroscopy with an attenuated total reflection accessory in the range of 4000 to 500 cm^{-1}.

To evaluate the flexural and compressive properties of PEEK composites, the testing specimens were prepared using a mini-injection molding machine (Bautek Co., Uijeongbu-si, Korea) at processing temperatures of 390 ℃. The

mold temperature was set to 200 ℃. The composite powders were molded into 80 × 10 × 4 mm^3 and 10 × 10 × 4 mm^3 plates for flexural and compressive tests, respectively. The composite specimens were annealed at 220 ℃ for 4 hr to improve crystallinity and reduce thermal stress. The flexural and compressive properties were measured with a universal testing machine (UTM, LR10K, Lloyd, West Sussex, UK) according to the ISO 178 and ISO 604 standards, respectively. 10 kN of load cell was used for both tests. The cross-head speeds were 2.0 mm/min for flexural test and 1.0 mm/min for compression tests. The average of five measurements was obtained from seven specimens for each test.

The fracture surface of composites after flexural testing was characterized by SEM. The morphology and dispersion state of the HA, m-HA, HANF, and m-HANF in the composites were observed by X-ray tomography microscope system (XRM, Xradia 620 Versa, ZEISS). The dimensions of monitored specimens were 0.4 × 0.4 × 0.4 mm^3. The X-ray source was operated at a voltage of 42 kV and a current of 240 μA. The XRM images of the composites were obtained by reconstructing the projections using software (Dragonfly) for three-dimensional modeling.

2.3. Results and discussion

Characterization of HANF

The morphology of the synthesized HANF was shown in **Figure 2.3**. The average diameter and length of synthesized HA nanofibers were 500 nm and 20 μm, respectively. The aspect ratio of HANF was about 40. In **Figure 2.4**, XRD and FTIR spectra were investigated to identify the chemical structure of synthesized HANF. The XRD patterns of the synthesized HANF were presented in **Figure 2.4 (a)** and **2.4 (b)**. According to the phase analysis, the sample showed same bands observed for the carbonated HA [22,23]. The crystallinity of the HANF was calculated by following equation [24]:

$$X_c = 1 - (V_{112/300}/I_{300})$$

where $V_{112/300}$ is the intensity of the hollow between (112) and (300) reflections and I_{300} is the intensity of (300) reflection. The calculated crystallinity of the synthesized HANF was 82%.

As shown in **Figure 2.4 (c)** and **2.4 (d)**, the FTIR spectrum of synthesized HANF was similar to the reported FTIR data for the carbonated HA [25,26]. HANF presented the asymmetric stretching vibrations of P–O groups at 1089 cm^{-1} and 1010 cm^{-1}. The characteristic absorption peaks at 961 cm^{-1} and 600 cm^{-1} were corresponded to the symmetric stretching and in-plane bending of P–O groups, respectively. The peaks at 3568 cm^{-1} and 633 cm^{-1} corresponded to hydroxyl groups that were not substituted by CO_3 groups. The weak and broad band at 3330 cm^{-1} was assigned to absorbed water. The peak at 872 cm^{-1} was sourced from the bending of CO_3. The peaks at 1419 cm^{-1} and 1455 cm^{-1}

were attributed to the symmetric stretching of A type and B type CO_3, respectively. These results indicate that the synthesized HANF in this study was AB-type carbonated HA.

Surface modification of fillers

In order to confirm the surface modification of HA, HANF, and CF, the chemical compositions of modified fillers were explored by XPS. **Figure 2.5** showed the XPS survey of m-HA, m-HANF, and m-CF. Before APTES and SAH treatment, the pristine HA and HANF (Figure 2.5a) exhibited peaks of O1s (531.1 eV), Ca2s (439.1 eV), Ca2p (347.1 eV), C1s (285.1 eV), P2s (190.1 eV), and P2p (133.1 eV), which agreed with the reported XPS data for the HA [27]. After the surface modification, the new peaks of N1s (399.1 eV), Si2p (153.1 eV), and Si2s (102.1 eV) appeared due to the surface treatment with APTES. Moreover, the high resolution spectra of N element showed in **Figure 2.5 (c)** and **2.5 (d)** revealed three peaks of free amine group at 399.1 eV (13.8% for m-HA and 14.7% for m-HANF), amide group at 400.3 eV (74.2% for m-HA and 70.6% for m-HANF), and protonated amine group at 401.7 eV (12.0% for m-HA and 14.7% for m-HANF). The protonated amine was originated from the interaction of amine groups with each other or with unreacted silanol groups of the substrate [28]. The high percentage of amide group indicated that the majority of amine end groups were successfully modified to carboxyl end groups by reaction with succinic anhydride.

As shown in **Figure 2.5 (b)**, the neat CF only exhibited peaks of O1s (532.1 eV) and C1s (285.1 eV). After the surface modification, m-CF showed

the new N1s (400.1 eV), Si2p (154.1 eV), and Si2s (103.1 eV) peaks due to the addition of N and Si elements from APTES. The N1s spectra for m-CF (**Figure 2.5 (e)**) were peak-fitted to 399.1 eV (12.3%), 400.4 eV (73.4%), and 401.9 eV (14.3%), attributed to amine, amide, and protonated amine groups, respectively [29]. These results confirmed that the majority of end groups of the surface-treated fillers were modified to carboxyl end groups.

PEEK/HA/CF composites

The flexural properties and the compressive strength of PEEK/HA/CF and PEEK/m-HA/m-CF composites were shown in **Table 2.3**. Overall, by the addition of HA and m-HA, the flexural strength and strain at break were decreased with increasing concentration as shown in **Figure 2.6**. For instance, the flexural strength of H1 was decreased by 26% from 157 MPa of neat PEEK to 116 MPa, whereas the flexural strength of H2 was decreased by 42% from 157 to 91 MPa. Such decrease in the flexural strength and strain at break of H1 and H2 were mainly caused by the aggregation of HA filler. As shown in **Figure 2.7**, the flexural modulus was increased with increasing content of HA due to reduction in the elastic resistance by the lamellar microcrystals formed between the HA particles and the PEEK matrix [11]. On the other hand, m-H1 sample showed similar flexural strength value within the error range compared to the flexural strength of neat PEEK sample. Moreover, the flexural strength of m-H2 was only decreased by 4.5% from 157 to 150 MPa, indicating enhanced dispersibility of HA particles in the matrix and improved

bonding strength between HA particles and the PEEK polymer chain. The flexural strain at break and the flexural modulus were also enhanced after the addition of m-HA. The role of coupling agent in the composites is not only to improve the dispersion of filler by reducing the surface energy but also to form an interface layer between filler and matrix polymer. The interface layer can enhance the bonding strength by transferring stress, thus improving the mechanical properties of composites [30,31].

Overall, both flexural strength and modulus were improved as the CF content increased due to the high modulus and stiffness characteristics of the CF filler [32]. The flexural strength and modulus of PEEK/CF composite was highest in C3 sample increased by 60% from 157 to 251 MPa and 365% from 3.7 to 13.5 GPa, respectively. Meanwhile, the rigid characteristics of CF filler caused the reduction in the flexural strain at break with increasing the content. After the addition of m-CF, the flexural strength and modulus were further enhanced as shown in **Figure 2.6** and **2.7**, respectively. For instance, the flexural strength and modulus of m-C3 sample were increased by 64% from 157 to 258 MPa and 421% from 3.7 to 15.6 GPa, respectively. The flexural modulus of m-C3 sample found to match the elastic modulus value of human cortical bone, which is about 14 GPa. The flexural strain of PEEK/m-CF composites was not dramatically increased compared to the result of PEEK/m-HA composites. The interfacial interaction and dispersion of HA particles in the PEEK matrix were improved simultaneously by the surface modification of HA. However, the enhancement in the interfacial interaction of CF with PEEK by surface modification was the main factor for the

improvement in mechanical properties because micro-sized CF filler was generally well dispersed in the composites without any surface modification.

For the flexural properties of PEEK/HA/CF composites, similar trends were observed as for PEEK/HA and PEEK/CF composites. As shown in **Figure 2.6** and **2.7**, the flexural strength and modulus were highest in m-H1C3 sample increased by 65% from 157 to 260 MPa and 486% from 3.7 to 18.0 GPa, respectively. The flexural strength of m-H1C3 was found to be slightly above the flexural strength of cortical bone that ranged from 103-238 MPa [33]. The flexural strain at break value of m-H1C3 (2.1%) was within the range of cortical bone (1 to 3%) [34]. Even though the flexural strength was decreased as the content of m-HA was increased to 20 wt%, the flexural strength m-H2C2 was found to match the middle range of cortical bone. Moreover, both flexural modulus and strain at break were well matched to the values of cortical bone.

Table 2.4 showed the compressive strength of PEEK/HA/CF composites. Overall, the compressive strength of PEEK composite was enhanced by the addition of HA and CF fillers. As shown in **Figure 2.8**, the compressive strengths of H2 and C3 were increased by 11% from 120 to 134 MPa and 28% from 120 to 166 MPa, respectively. Such increase in the compressive strength was due to dense structure of HA particles and high mechanical properties of CF fillers. When the surface modified fillers were used, the compressive strengths were further improved because of enhanced interfacial interaction between filler and PEEK matrix. For instance, the compressive strengths of m-H2 and m-C3 were enhanced by 16% from 120 to 142 MPa and 30% from

120 to 171 MPa, respectively. The highest compressive strength was achieved by H1C3 composite (191 MPa), which found to be in the high range of cortical bone (106 to 215 MPa) [35].

In **Figure 2.9**, the dispersion of HA particles in PEEK matrix was analyzed by XRM. Before any surface treatment, HA fillers showed severe agglomerations. For example, HA aggregates that are larger than 200 μm were easily observed in the H1 sample as shown in **Figure 2.9 (a)**. In contrast, the m-H1 sample in **Figure 2.9 (b)** showed much improved dispersion of HA particles after surface modification. The biggest size of m-HA aggregate was about 25 μm, and the average size was $\leq$5 μm. When the content of m-HA particles was increased to 20 wt% (**Figure 2.9 (c)**), the size of m-HA aggregates was slightly increased again, indicating re-aggregation of m-HA particles. These results imply that the surface modification of HA particles could enhance the dispersibility of HA filler, thereby improving both flexural and compressive strength of the PEEK/HA/CF composite.

As shown in **Figure 2.10**, the fracture morphologies of PEEK/HA and PEEK/CF composites after flexural testing were obtained to investigate the effect of surface modification on the dispersibility of fillers and the interfacial interaction between filler and matrix. Overall, the fracture surface of composites showed brittle failure while neat PEEK usually showed ductile failure. When the unmodified HA was added, HA particles were severely aggregated as shown in **Figure 2.10 (a)**. The HA particles in H1 composite showed particulate de-bonding by poor interfacial adhesion with the PEEK matrix, resulting early fracture of composite. Thus, the reduction in flexural

strength of H1 and H2 composites was due to the aggregation of HA and poor interface between HA particles and PEEK matrix. However, m-H1 showed a decrease in size of HA aggregates as shown in **Figure 2.10 (b)**. And, the interfacial interaction between PEEK polymer chains and m-HA particles were enhanced after surface modification. The improvement in interfacial adhesion between m-HA and PEEK was thought to be due to hydrogen bonding between the carboxylic groups of m-HA as donor and the ketone groups of PEEK as acceptor. However, when the content of m-HA was increased to 20 wt%, the size of the HA aggregate was observed to increase again.

Figure 2.10 (d) and **2.10 (e)** showed the fracture morphologies of C1 and m-C1 composites after flexural testing. The voids between CF and PEEK matrix in C1 composite indicated poor interfacial adhesion (**Figure 2.10 (d)**), whereas the gaps between m-CF and PEEK matrix were not observed as shown in **Figure 2.10 (e)**. The polymer chains were well attached onto the m-CF surface, providing extra resistance against the external stress. Thus, both flexural and compressive strength of PEEK/m-CF composites could be increased. Furthermore, m-H1C1 composite reinforced with m-HA and m-CF showed similar morphology to the m-H1 and m-C1 composites. The aggregation of HA particles was mitigated, and the interface gaps between the CF filler and the PEEK matrix was minimized.

PEEK/HANF/CF composites

The flexural properties and the compressive strength were shown in **Table**

2.4. While the flexural strength of H1 composite was decreased, the flexural strength of HF1 composite was increased by 14% from 157 to 180 MPa. When the content of HANF was increased to 20 wt%, the flexural strength of HF2 was decreased similarly to that of H2 due to the aggregation of HANF. But, the reduction was not as large as in the H2 composite. This was due to the bridging effect of the fibers, which slows down the delamination growth and increases the resistance to the crack growth [36]. In addition, nanofibers were expected to reduce agglomeration due to a lower surface area compared to HA nanoparticle. Thus both flexural modulus and stain at break could be enhanced compared to the results of PEEK/HA composites. **Figure 2.11** and **2.12** showed the flexural strength and modulus, respectively, of PEEK composites reinforced by surface modified HANF and CF. After surface modification of HANF, the flexural strength of all composite samples was increased due to the improved interfacial adhesion between HANF and PEEK matrix. The flexural strength and modulus were highest in m-HF1C3 sample, increased by 68% from 157 to 264 MPa and 505% from 3.7 to 18.7 GPa, respectively. The results of flexural strain at break were also increased after the addition of m-HANF due to enhanced dispersion and interfacial adhesion.

By the addition of HANF and CF, the compressive strength was increased with increasing concentration. As shown in **Figure 2.13**, the compressive strengths of HF2 and HF1C3 were enhanced by 15% and 57%, respectively. Overall, PEEK/HANF/CF composites showed higher compressive strength than PEEK/HA/CF composites mainly due to good dispersion and high aspect ratio. When the modified HANF and CF were used, the compressive strength

was further improved. For instance, the highest compressive strength was achieved by m-HF1C3 (203 MPa) and m-HF2C2 (202 MPa), which found to be in the high range of cortical bone (106 to 215 MPa).

Figure 2.14 showed the dispersion of HANF and m-HANF in HF1, m-HF1, and m-HF2 composites. For HF1 composite (**Figure 2.14 (a)**), the XRM analysis showed that the size of HANF aggregates was about 20 to 30 μm, which was similar to the result of m-H1 composite. The HANF particles were dispersed relatively well without any surface modification. This improvement in dispersion was the main reason for the increase in flexural strength of HF1 composite. However, the dispersion of HANF was further improved after surface modification as shown in **Figure 14 (b)**. The m-HANF particles were dispersed well and uniformly in the PEEK matrix, resulting in higher mechanical strength. When the content of m-HANF was increased to 20 wt% (**Figure 2.14 (c)**), the size of m-HANF were increased, similar to the result of m-H2 composite. This was the main reason for the reduction in flexural strength of m-HF2.

Figure 2.15 showed the fracture morphologies of HANF and m-HANF reinforced PEEK composites after flexural testing. Compared to the fracture morphologies of H1 (**Figure 2.15 (a)**), HF1 showed much improved dispersion of HANF. However, the voids between HANF and PEEK matrix were easily observed at high magnification. The addition of m-HANF particles significantly reduced the voids between m-HANF and the PEEK matrix, improving the interfacial strength. Thereby, the mechanical strength of m-HANF reinforced PEEK composites could be increased. When the content

of HANF or m-HANF was increased to 20 wt%, HF2 showed strong aggregation of HANF particles and m-HF2 showed small aggregation of m-HANF particles. This was the main reason for the decrease in flexural properties of HANF or m-HANF reinforced PEEK composites. Similar to the fracture morphology of m-H1C1 composite, m-HF1C1 composite also showed a well dispersed m-HANF and m-CF fillers and good interfacial adhesion between the fillers and the PEEK matrix.

2.4. Conclusion

PEEK/m-HA/m-CF and PEEK/m-HANF/m-CF composites were successfully produced with the addition of surface modified HA, HANF, and CF fillers. When the modified fillers were added to the PEEK composite, both flexural properties and compressive strength were improved, up to a bone-like modulus and strength. The XRM analysis showed that the dispersion of HA particles in the PEEK matrix was enhanced after surface modification. The SEM result confirmed the improvement in interfacial adhesion between the fillers and the PEEK matrix after surface modification due to hydrogen bonding between m-HA and PEEK. When the synthesized HANF was used instead of HA, the mechanical properties further improved by bridging effect of the fiber and high aspect ratio. Moreover, the implementation of HANF in PEEK polymer matrix suggested the possibility that the dispersibility of other nanofibers can be also improved by using nanofibers with higher stiffness due to less entanglement during the blending process. Like m-HA in PEEK/m-HA/m-CF composite, m-HANF also showed the improvement in interfacial adhesion with PEEK matrix. Overall, the PEEK/m-HANF/m-CF composite showed higher mechanical properties than the PEEK/m-HA/m-CF composite. Moreover, the mechanical properties of PEEK/m-HANF/m-CF composite such as m-HF1C3 showed similar values to those of cortical bones, thus PEEK/m-HANF/m-CF composite is expected to be used as a material for spinal implants.

Table 2.1. Blend formulations of PEEK/HA/CF composite samples.

Designation	PEEK content (wt%)	HA content (wt%)	CF content (wt%)
PEEK	100	0	0
H1	90	10	0
H2	80	20	0
C1	90	0	10
C2	80	0	20
C3	70	0	30
H1C1	80	10	10
H1C2	70	10	20
H1C3	60	10	30
H2C1	70	20	10
H2C2	60	20	20

Table 2.2. Blend formulations of PEEK/HANF/CF composite samples.

Designation	PEEK content (wt%)	HANF content (wt%)	CF content (wt%)
PEEK	100	0	0
HF1	90	10	0
HF2	80	20	0
HF1C1	80	10	10
HF1C2	70	10	20
HF1C3	60	10	30
HF2C1	70	20	10
HF2C2	60	20	20

Table 2.3. Mechanical properties of PEEK/HA/CF composites.

	Flexural Modulus (GPa)		Flexural Strain at Break (%)		Flexural Strength (MPa)		Compressive Strength (MPa)	
	Unmodified	Modified	Unmodified	Modified	Unmodified	Modified	Unmodified	Modified
PEEK	3.7 ± 0.1		-		157 ± 2		120 ± 2	
H1	4.4 ± 0.1	4.5 ± 0.1	2.9 ± 0.1	5.0 ± 0.1	116 ± 3	155 ± 2	127 ± 3	131 ± 2
H2	4.8 ± 0.1	5.4 ± 0.1	2.2 ± 0.1	3.4 ± 0.2	91 ± 5	150 ± 4	134 ± 4	142 ± 2
C1	5.6 ± 0.1	6.3 ± 0.1	5.2 ± 0.3	5.6 ± 0.3	182 ± 3	194 ± 4	135 ± 1	140 ± 2
C2	8.7 ± 0.1	10.6 ± 0.3	3.5 ± 0.2	3.6 ± 0.2	219 ± 3	232 ± 2	150 ± 1	156 ± 2
C3	13.5 ± 0.4	15.6 ± 0.5	2.4 ± 0.1	2.4 ± 0.2	251 ± 5	258 ± 3	166 ± 1	171 ± 2
H1C1	7.8 ± 0.1	7.7 ± 0.2	2.7 ± 0.1	3.9 ± 0.1	161 ± 4	190 ± 4	141 ± 2	152 ± 2
H1C2	11.1 ± 0.2	13.0 ± 0.2	2.4 ± 0.1	2.6 ± 0.1	209 ± 2	228 ± 2	156 ± 1	166 ± 3
H1C3	17.1 ± 0.3	18.0 ± 0.3	1.7 ± 0.1	2.1 ± 0.1	225 ± 4	260 ± 3	178 ± 1	191 ± 2
H2C1	9.0 ± 0.1	8.9 ± 0.2	1.6 ± 0.1	2.7 ± 0.1	131 ± 3	179 ± 5	149 ± 2	161 ± 2
H2C2	13.4 ± 0.2	14.5 ± 0.2	1.4 ± 0.1	1.7 ± 0.1	164 ± 4	204 ± 3	161 ± 1	172 ± 1

Table 2.4. Mechanical properties of PEEK/HANF/CF composites.

	Flexural Modulus (GPa)		Flexural Strain at Break (%)		Flexural Strength (MPa)		Compressive Strength (MPa)	
	Unmodified	Modified	Unmodified	Modified	Unmodified	Modified	Unmodified	Modified
PEEK	3.7 ± 0.1		-		157 ± 2		120 ± 2	
HF1	5.8 ± 0.1	5.9 ± 0.2	5.9 ± 0.2	6.5 ± 0.3	180 ± 1	185 ± 2	138 ± 2	143 ± 2
HF2	6.8 ± 0.2	7.5 ± 0.1	3.2 ± 0.1	3.8 ± 0.1	169 ± 2	173 ± 2	145 ± 1	149 ± 1
HF1C1	8.1 ± 0.2	8.4 ± 0.1	3.7 ± 0.2	4.1 ± 0.2	200 ± 3	209 ± 3	153 ± 2	158 ± 1
HF1C2	12.4 ± 0.3	13.1 ± 0.2	2.5 ± 0.1	2.6 ± 0.2	223 ± 3	232 ± 3	171 ± 2	180 ± 1
HF1C3	18.0 ± 0.3	18.7 ± 0.2	1.8 ± 0.1	2.0 ± 0.1	241 ± 4	264 ± 3	188 ± 1	203 ± 1
HF2C1	10.9 ± 0.4	11.4 ± 0.4	2.2 ± 0.1	2.4 ± 0.1	188 ± 4	202 ± 3	165 ± 1	173 ± 2
HF2C2	16.0 ± 0.5	18.0 ± 0.4	1.7 ± 0.1	1.9 ± 0.1	214 ± 5	223 ± 3	183 ± 1	202 ± 2

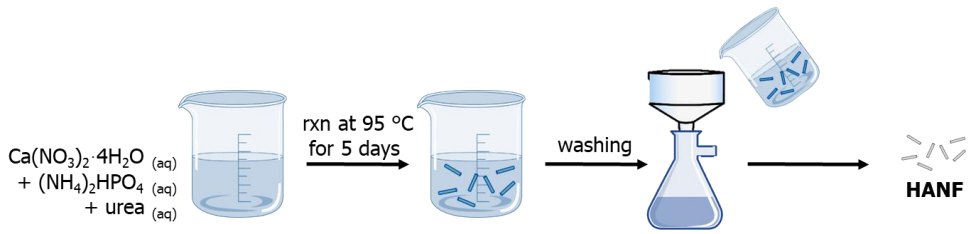

Figure 2.1. A schematic of HANF synthesis.

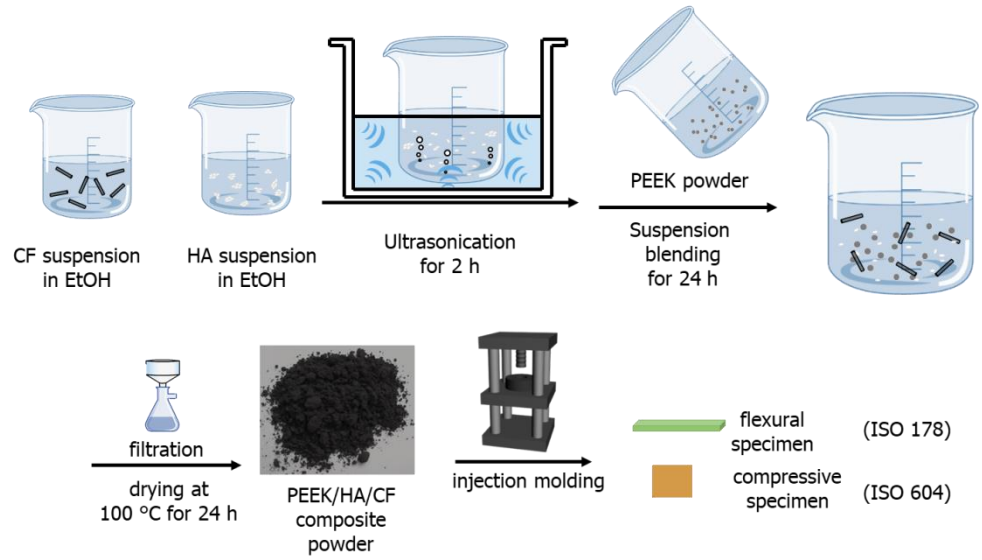

Figure 2.2. A schematic of suspension blending method to prepare PEEK composites.

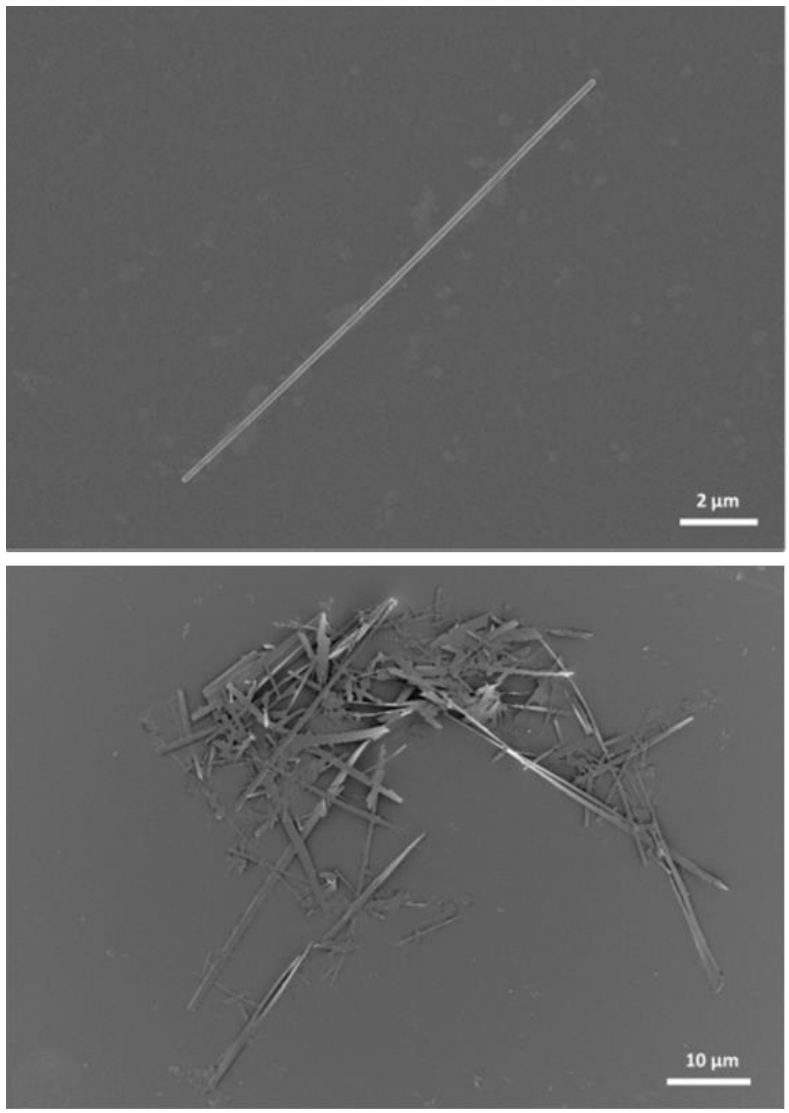

Figure 2.3. SEM images of synthesized HANF.

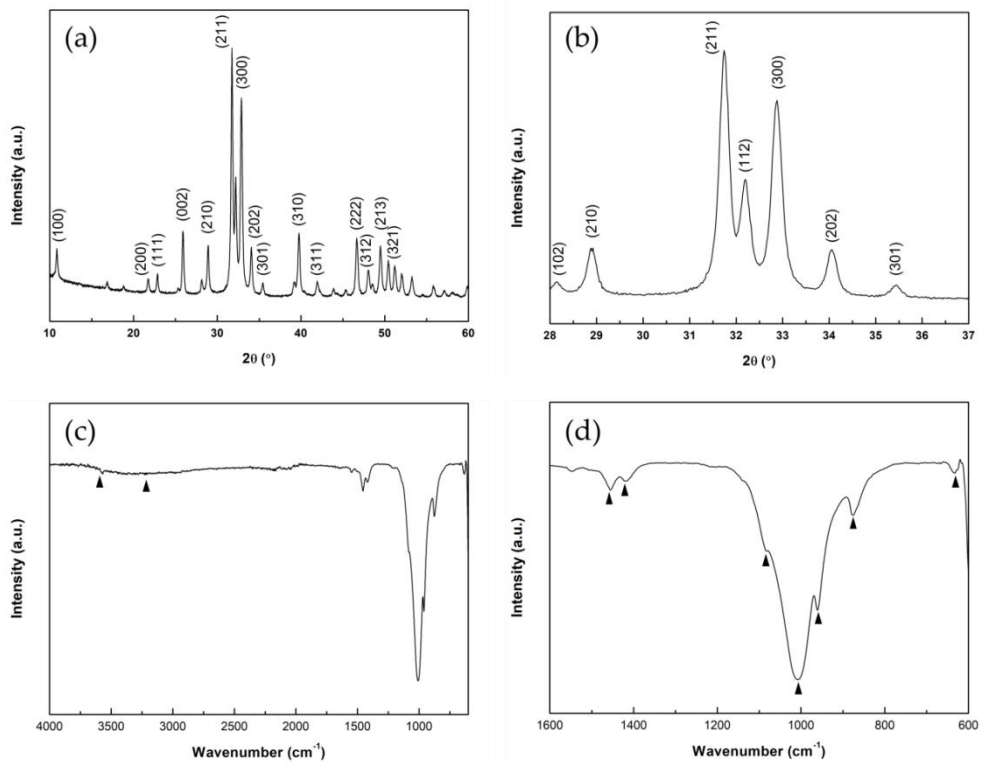

Figure 2.4. (a) XRD pattern and (b) magnified region of HANF; (c) FTIR spectrum and (d) magnified region of HANF.

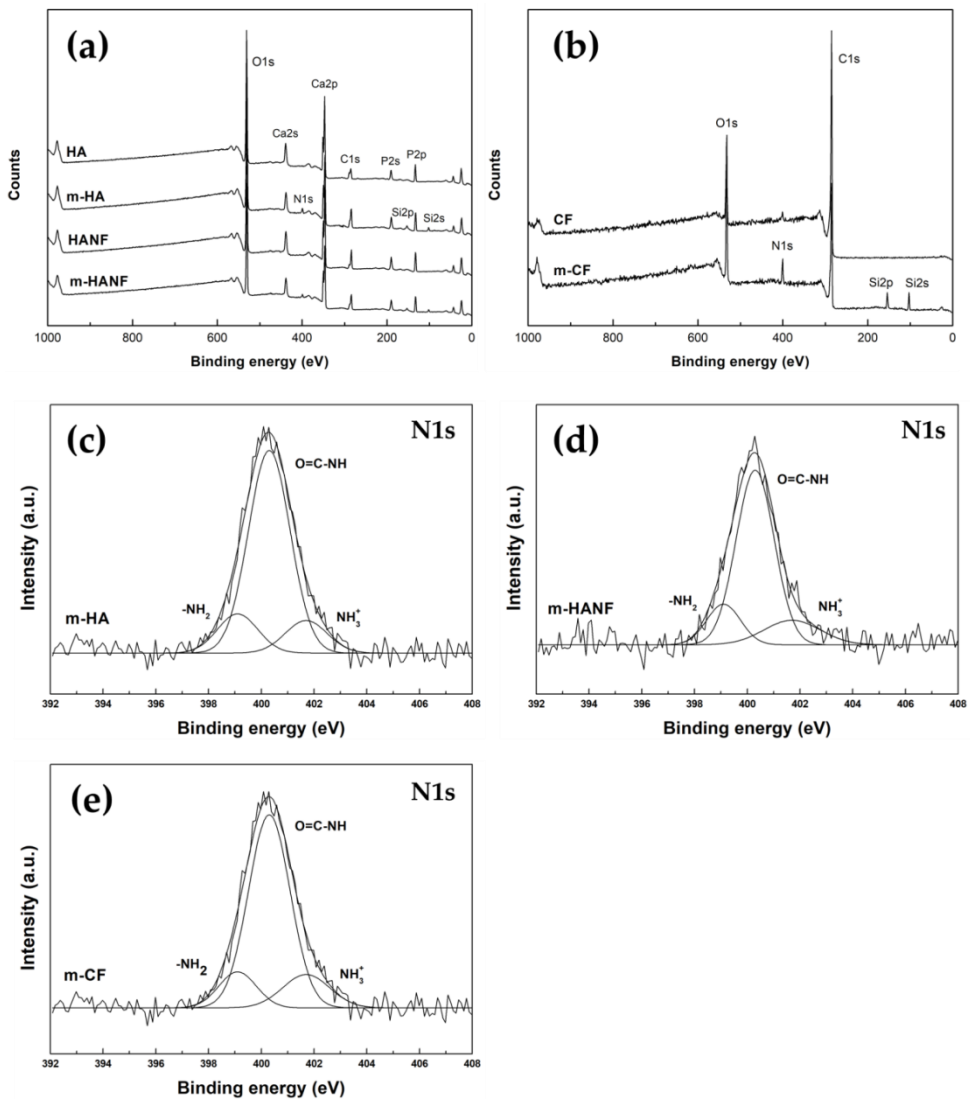

Figure 2.5. (a) XPS survey of HA, m-HA, HANF, and m-HANF; (b) XPS survey of CF and m-CF; XPS N1s spectra for (c) m-HA, (d) m-HANF, and (e) m-CF.

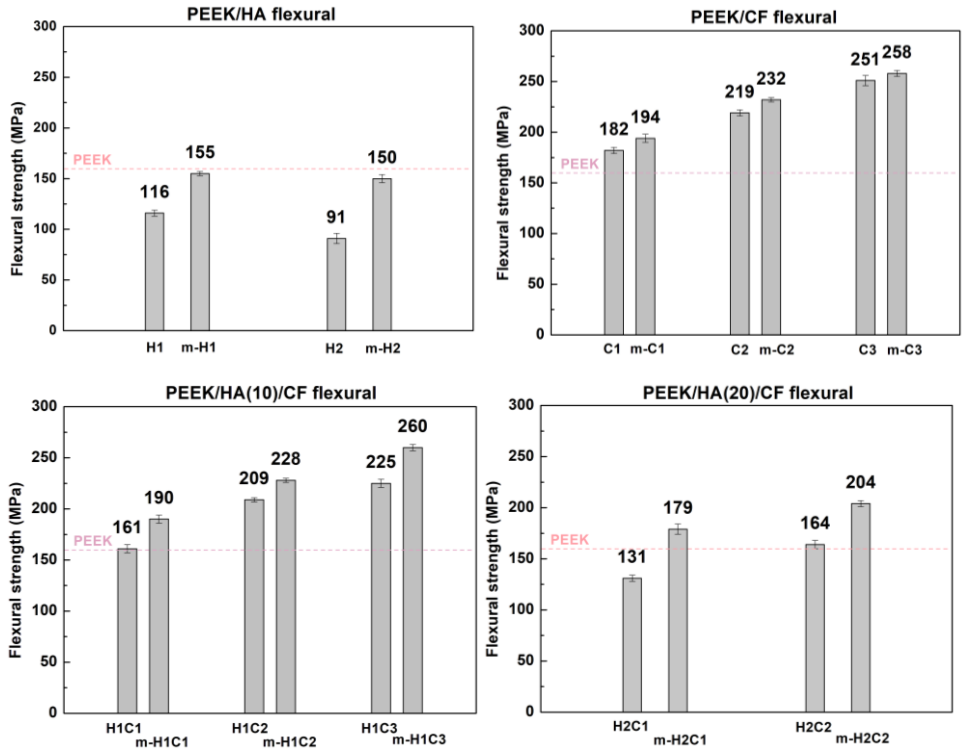

Figure 2.6. Flexural strength of PEEK composites with m-HA and m-CF.

.

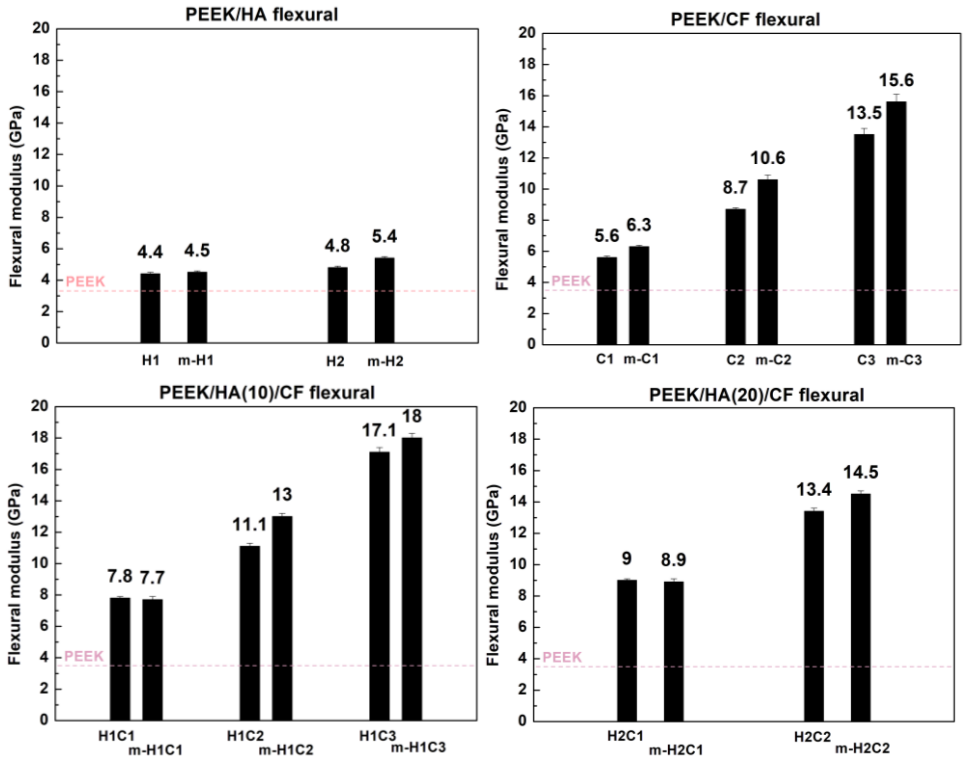

Figure 2.7. Flexural modulus of PEEK composites with m-HA and m-CF.

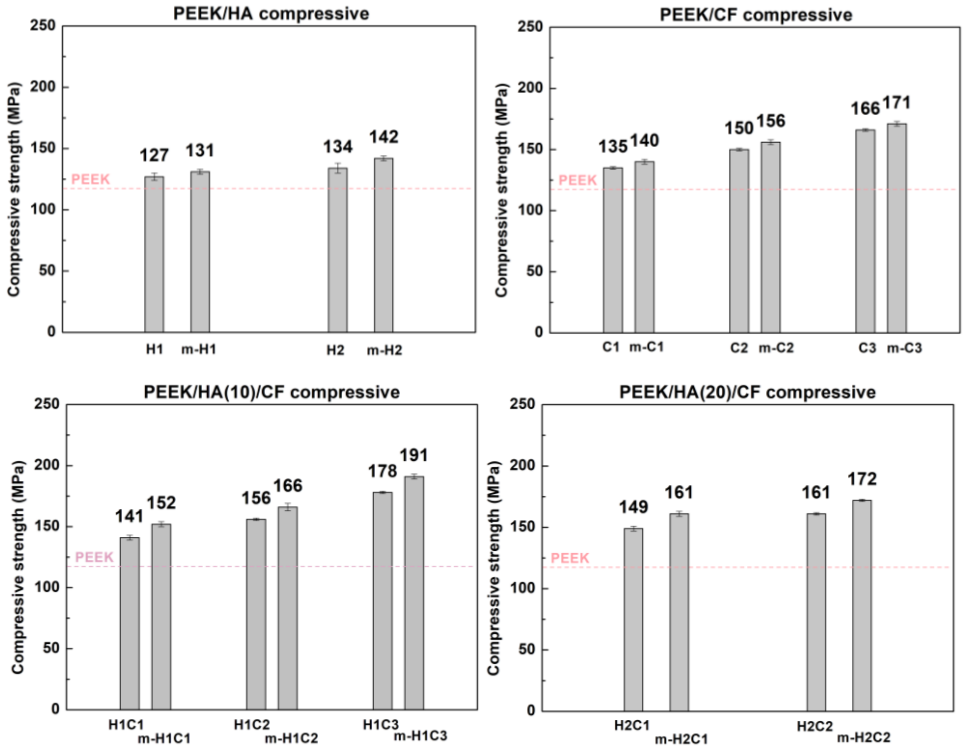

Figure 2.8. Compressive strength of PEEK composites with m-HA and m-CF.

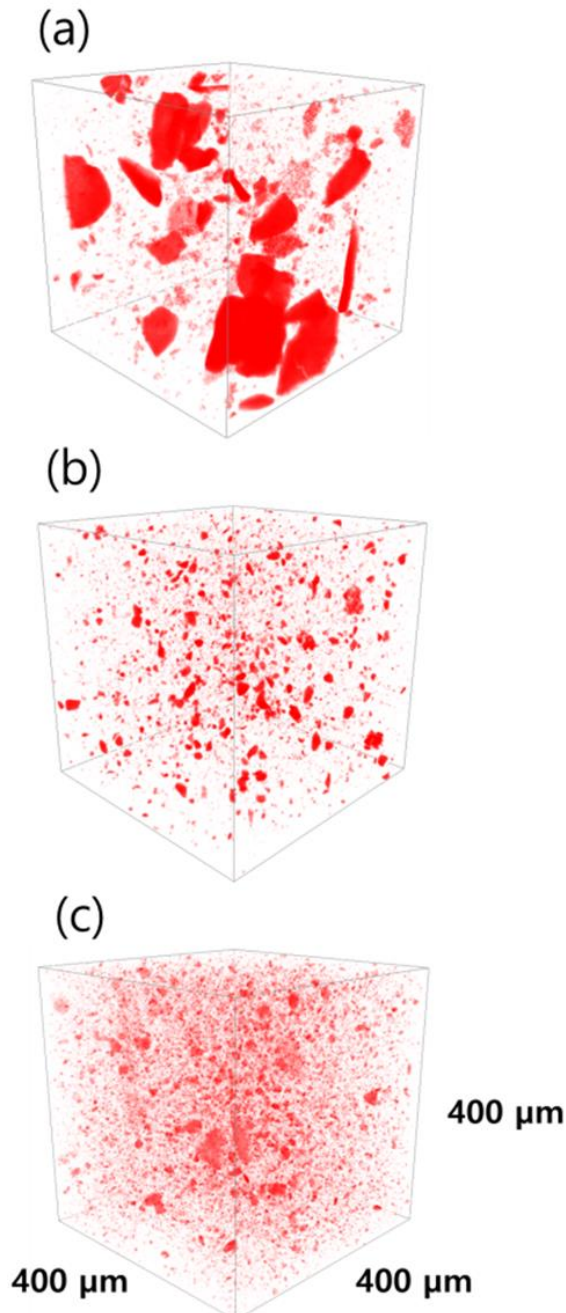

Figure 2.9. XRM analysis on (a) H1, (b) m-H1, and (c) m-H2 composites.

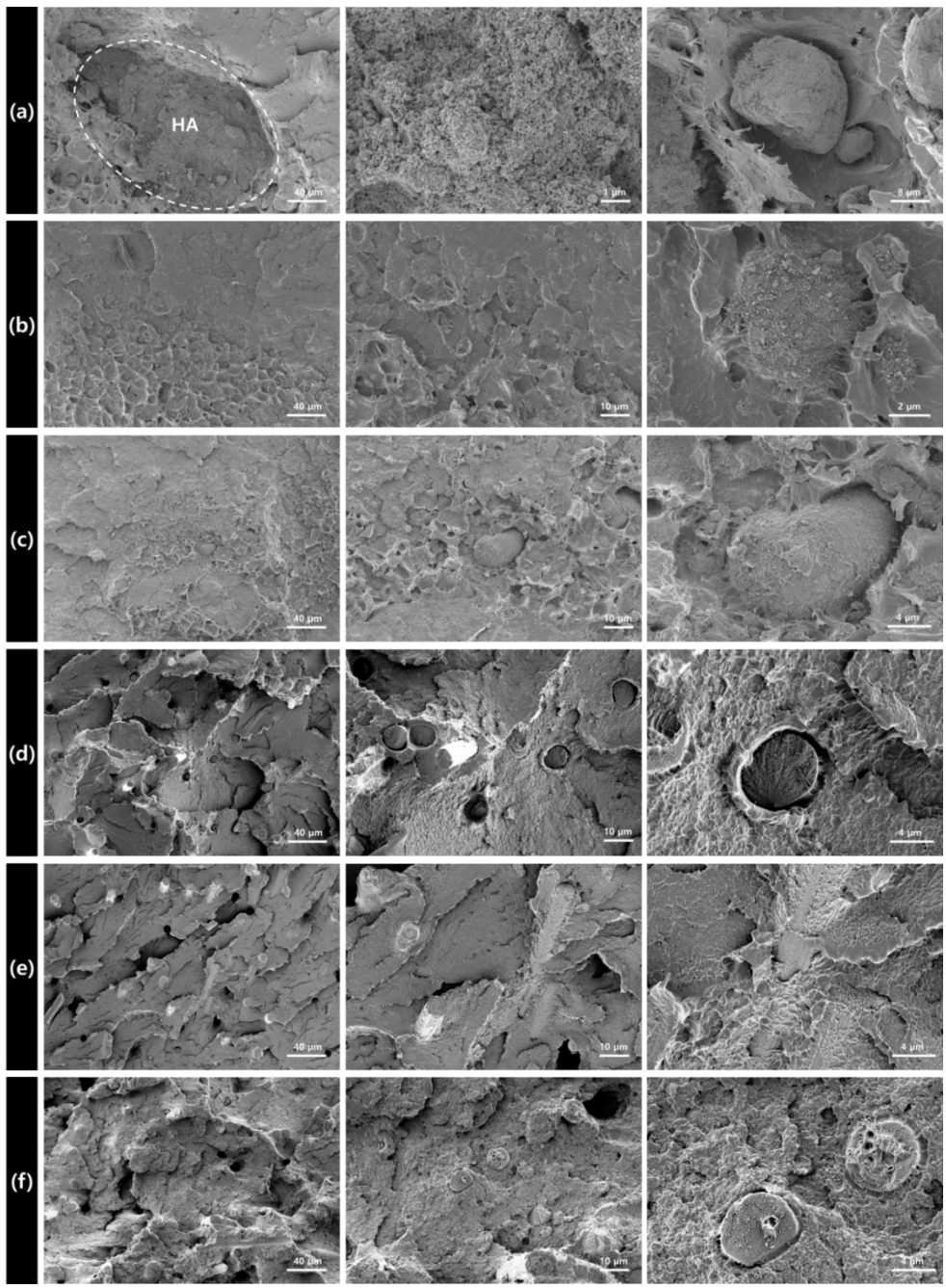

Figure 2.10. Fracture morphologies of (a) H1, (b) m-H1, (c) m-H2, (d) C1, (e) m-C1, and (f) m-H1C1 composites.

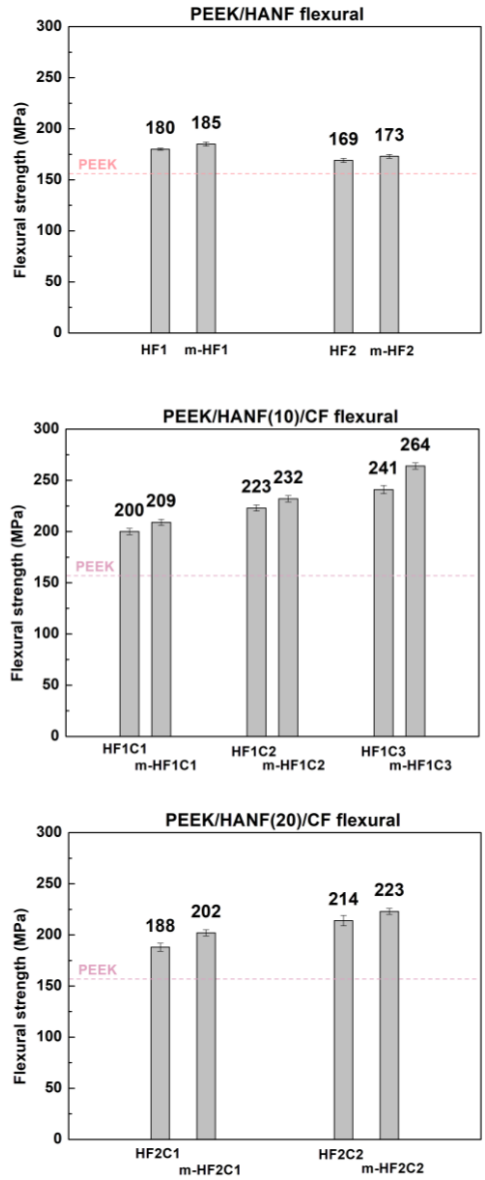

Figure 2.11. Flexural strength of PEEK composites with m-HF and m-CF.

.

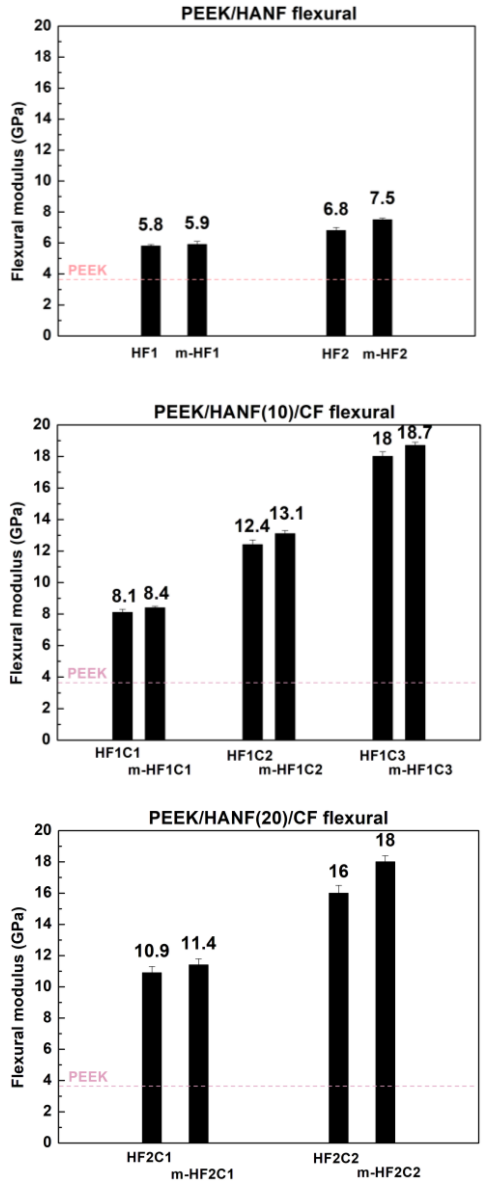

Figure 2.12. Flexural modulus of PEEK composites with m-HF and m-CF.

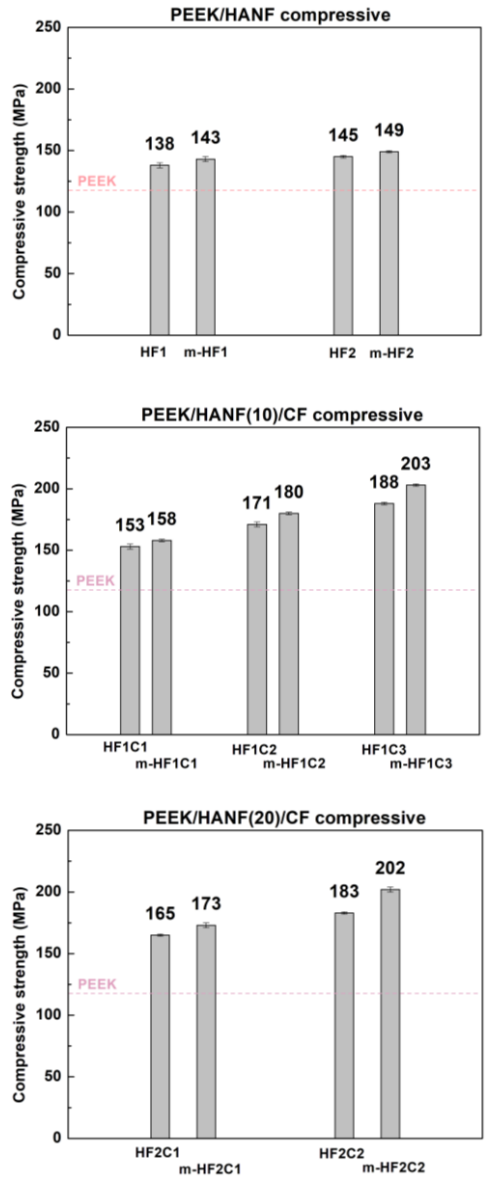

Figure 2.13. Compressive strength of PEEK composites with m-HF and m-CF.

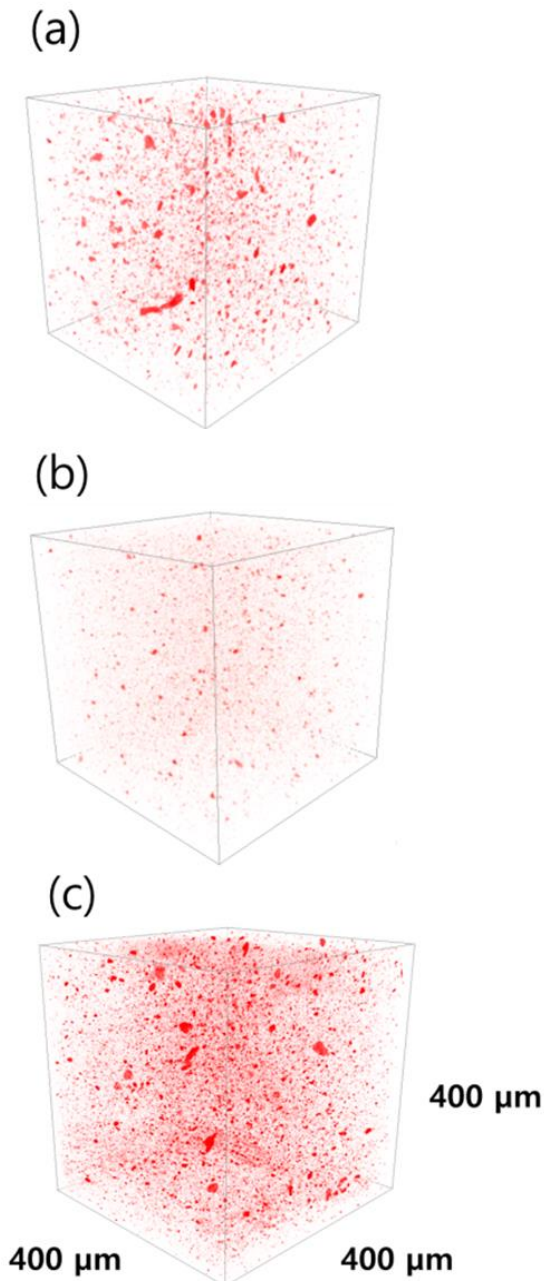

Figure 2.14. XRM analysis on (a) HF1, (b) m-HF1, and (c) m-HF2 composites.

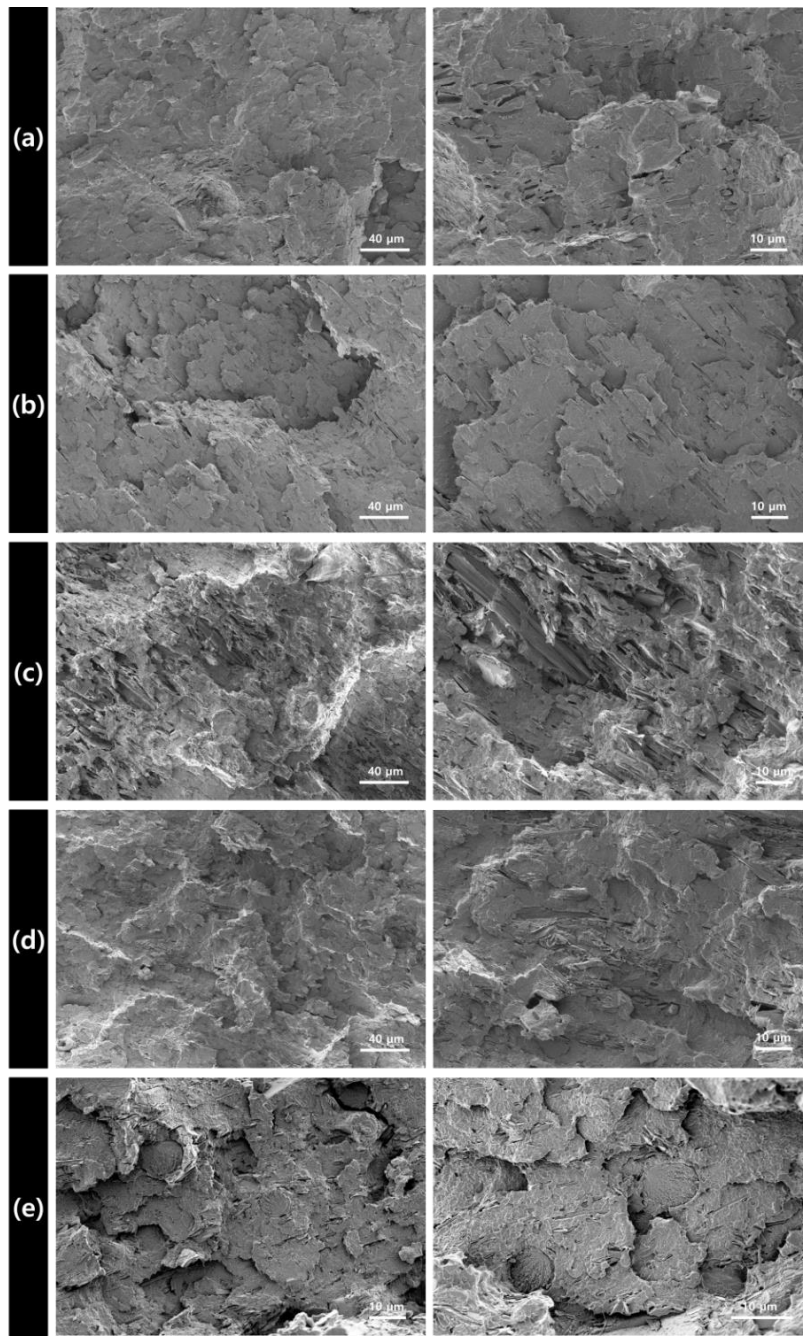

Figure 2.15. Fracture morphologies of (a) HF1, (b) m-HF1, (c) HF2, (d) m-HF2, and (e) m-HF1C1 composites.

2.5. References

[1] S. Huiskes, *R. Acta Orthop. Belg*., **1993**, *59*, 118.

[2] M. I. Z. Ridzwan, S. Shuib, A. Y. Hassan, A. A. Shokri, M. N. M. Ibrahim, M. N. Mohammad Ibrahim, *J. Med. Sci*., **2007**, *7*, 460.

[3] J. Y. Rho, R. B. Ashman, C. H. Turner, *J Biomech*., **1993**, *26*, 111.

[4] S. Mishra, R. Chowdhary, *Clin. Implant Dent. R*., **2019**, *21*, 208.

[5] S. M. Kurtz, J. N. Devine, *Biomaterials*, **2007**, *28*, 4845.

[6] C. S. Li, C. Vannabouathong, S. Sprague, M. Bhandari, *Clinical Medicine Insights: Arthritis and Musculoskeletal Disorders*, **2015**, *8*, 33.

[7] Y. Deng, P. Zhou, X. Liu, L. Wang, X. Xiong, Z. Tang, J. Wei, S. Wei, *Colloids Surf. B Biointerfaces*, **2015**, *136*, 64.

[8] X. Feng, G. Sui, R. Yang, *Chin. J. Mater. Res.*, **2008**, *22*, 18.

[9] M. N. Uddin, P. S. Dhanasekaran, R. Asmatulu, *Prog. Biomater.*, **2019**, *8*, 211.

[10] M. S. Abu Bakar, M. H. W. Cheng, S. M. Tang, S. C. Yu, K. Liao, C. T. Tan, K. A. Khor, P. Cheang, *Biomaterials*, **2003**, *24*, 2245.

[11] R. Ma, Q. Li, L. Wang, X. Zhang, L. Fang, Z. Luo, B. Xue, L. Ma, *Mat. Sci. Eng. C*, **2017**, *73*, 429.

[12] L. Wang, L. Q. Weng, Z. Z. Wu, C. B. Wang, *Adv. Mat. Res*., **2015**, *1096*, 214.

[13] A. R. Rashidi, M. U. Wahit, M. R. Abdullah, M. Rafiq, A. Kadir, *Adv. Mat. Res*., **2015**, *1125*, 426.

[14] J. Esmaeilzadeh, S. Hesaraki, S. M. M. Hadavi, M. H. Ebrahimzadeh, M. Esfandeh, *Mater. Sci. Eng. C*, **2017**, *77*, 978.

[15] S. Wang, S. Wen, M. Shen, R. Guo, X. Cao, J. Wang, X. Shi, *Int. J. Nanomedicine*, **2011**, *6*, 3449.

[16] S. Rakmae, Y. Ruksakulpiwat, W. Sutapun, N. Suppakarn, *Mater. Sci. Eng. C*, **2012**, *32*, 1428.

[17] K. G. Dassios, *Adv. Compos. Lett*., **2007**, *16*, 17.

[18] X. Tao, J. Liu, G. Koley, X. Li, *Adv. Mater.*, **2008**, *20*, 4091.

[19] L. Chen, Q. Yu, Y. Wang, H. Li, *Dent. Mater*., **2011**, *27*, 1187.

[20] H. -S. Ko, S. Lee, J. Y. Jho, *Nanomaterials*, **2021**, *11*, 213.

[21] H. Zhang, Y. Wang, Y. Yan, S. Li, *Ceram. Int.*, **2003**, *29*, 413.

[22] Z. Gandou, A. Nounah, B. Belhorma, A. Yahyaoui, *J. Mater. Environ. Sci.*, **2015**, *6*, 983.

[23] H. El Boujaady, M. Mourabet, A. EL Rhilassi, M. Bennani-Ziatni, R. El Hamri, A. Taitai, *J. Mater. Environ. Sci*., **2016**, *7*, 4049.

[24] Y. Sa, Y. Guo, X. Feng, M. Wang, P. Li, Y. Gao, X. Yang, T. Jiang, *New J. Chem*., **2017**, *41*, 5723.

[25] J. J. Lovón-Quintana, J. K. Rodriquez-Guerrero, P. G. Valença, *APPL CATAL A-GEN*, **2017**, *542*, 136.

[26] O. Kaygili, C. Tatar, F. Yakuphanoglu, *Ceram. Int*., **2012**, *38*, 5713.

[27] J. Yao, Y. Zhang, Y. Wang, M. Chen, Y. Huang, J. Cao, W. Ho, S. C. Lee, *RSC Adv*., **2017**, *7*, 24683.

[28] F. Zhang, M. P. Srinivasan, *Langmuir*, **2004**, *20*, 2309.

[29] N. Graf, E. Yegen, T. Gross, A. Lippitz, W. Weigel, S. Krakert, A. Terfort, W. E. S. Unger, *Surf. Sci*., **2009**, *603*, 2849.

[30] N. Pramanik, S. Mohapatra, P. Bhargava, P. Pramanik, Mater. *Sci. Eng. C*, **2009**, *29*, 228.

[31] C. Shuai, L. Yu, P. Feng, C. Gao, S. Peng, *Colloids Surf. B*, **2020**, *193*, 111083.

[32] P. Bhatt, A. Goel, *Mater. Sci. Res. India*, **2017**, *14*, 52.

[33] J. R. Caeiro, P. González, D. Guede, Rev. Osteoporos. *Metab. Miner*., **2013**, *5*, 99.

[34] M. Wang, D. Porter, W. Bonfield, *Br. Ceram. Trans*., **1994**, *93*, 91.

[35] A. C. Lawson, J. T. Czernuszka, *Proc. Instn. Mech. Engrs.- Part H*, **1998**, *212*, 413.

[36] A. Russo, M. Zarrelli, A. Sellitto, A. Riccio, *Materials*, **2019**, *12*, 2407.

Chapter 3

Mechanical Properties of Polyetheretherketone/hydroxyapatite/carbon fiber Composite prepared by Mechanofusion Process

The results described in this part have been published in *Polymers. 2021 June 13(12): 1978*

3.1. Introduction

In spinal cage applications, metals such as titanium (Ti) and stainless steel have been widely used for metallic implants due to their excellent corrosion resistance, biocompatibility, mechanical strength, and friction resistance. For example, Ti-6Al-4V, one of the titanium alloys, exhibits outstanding biocompatible and corrosion resistance [1]. However, mismatches in the Young's modulus, magnetic image interference, and release of ions are major issues [2]. Glass-ceramics such as Apatite-Wollastonite (A-W) are also used in the spinal cage application due to their good biocompatibility, low cost, and ware resistance. However, the use of A-W glass-ceramic is often limited because of its brittleness and poor handling properties [3,4].

A large number of polymers such as polyethylene (PE), polyethylene terephthalate (PET), polysulfone (PS), poly(lactic acid) (PLA), and poly(glycolic acid) (PGA) have been used in specific biomedical applications [5]. Nevertheless, these polymers are not suitable for use as a spinal cage application due to their low mechanical strength and modulus. Thereby, polyetheretherketone (PEEK) has been a primary candidate to replace metallic implants because of its good chemical resistance, biocompatibility, mechanical strength, and MRI compatibility [6–8]. While metallic implants often result in bone resorption and osteonecrosis due to a stress-shielding effect [9,10] from a much higher Young's modulus (102 to 110 GPa) than that of the natural human bone (~14 GPa), PEEK has a similar Young's modulus (3 to 4 GPa) to human bone and mitigate these issues [11–13].

Nonetheless, PEEK needs some improvements to be used in a spinal cage

application. Since the mechanical strength and elastic modulus of PEEK itself is in the low range of human cortical bone, PEEK should be further reinforced to match up with the mechanical properties of cortical bone. Carbon fiber (CF) is commonly used as a reinforcement in PEEK composite due to its excellent mechanical properties, biocompatibility, wearability, non-toxicity, and low cost [14,15]. Carbon fiber-reinforced PEEK (CFRPEEK) is currently used in the orthopedic field for various applications such as spinal cage, joint replacement, and plates [16]. In terms of mechanical properties, the higher the CF content in the composite, the better it is. However, the maximum content of CF in the composite should be adjusted due to the hydrophobicity, which can weaken the cell attachment, spreading, and proliferation [17]. Sandler et al. [13] reported that the tensile stiffness and strength of a PEEK composite can be enhanced by the addition of carbon nanofibers (CNF) due to increased surface area and energy of filler. In addition to CF, several studies in the literature have investigated the effect of various nanoparticles on the mechanical properties of PEEK. For example, Hwang et al. [18] improved the bending elastic modulus and damping properties of PEEK with the addition of graphene oxide (GO) and carbon nanotube (CNT). The friction and wear properties of PEEK also could be enhanced by the addition of GO [19]. However, in some cases, the nanoparticle-like graphene nanoplatelet can form an aggregation that can reduce the mechanical strength of PEEK composites [20].

Another factor that must be improved is bioactivity. Even though PEEK is a biocompatible polymer, it does not osseointegrate in vivo and does not provoke interactions with bone tissue [21]. In order to improve the bioactivity of PEEK, one of the bioactive ceramics that has been commonly used is hydroxyapatite (HA), a

bioactive calcium phosphate that has a similar chemical composition to human bone. HA is known to promote osteoblast adhesion and cell proliferation by its osteoconductive abilities [22–24]. However, nano-sized HA filler within the PEEK/HA composite can be easily agglomerated with increasing content due to its good hydrophilicity and high surface area [25,26]. In addition, aggregation of the HA filler leads to a severe reduction in mechanical strengths and modulus.

Many studies have reported different methods to improve the dispersibility of the HA nanoparticles in the polymer matrix. Mathieu et al. [27] produced a homogeneous dispersion of the HA in the PLA composite by the melt-extrusion method, but pointed out the risk of polymer degradation. An internal mixer (Haake) is another way to disperse nanoparticles in the composite by mechanical mixing force [28]. The dispersibility of HA also can be improved by modifying HA with the silane coupling agent. Ma et al. [29] reported that the surface-modified HA enhanced the tensile strength of the PEEK/HA composite by improving the dispersibility of HA and the interfacial adhesion between the HA and PEEK matrix. Wang et al. [2] developed a PEEK composite with nanofluorohydroxyapatite (FHA). Their results show FHA filler not only increased the elastic modulus and tensile strength similar to those of human cortical bone but also enhanced bioactivity, osseointegration, and bone–implant contact in vivo.

Some recent studies have been conducted involving HA and CF fillers incorporated in the PEEK matrix, as PEEK/HA/CF ternary composite in order to improve both the mechanical properties and bioactivity at the same time [17,30]. Even though PEEK/HA/CF ternary composite was enhanced in both mechanical properties and biological performances compared to pure PEEK matrix,

dispersibility of fillers in ternary composite was a major issue that has to be improved. In other words, the content of CF in ternary composite should be adjusted at the level of mechanical properties similar to bones, whereas the content of HA should be limited in a way that mechanical properties are not severely deteriorated due to aggregation.

A common method for PEEK composite fabrication in industrial fields is the melt-processing method using an extruder equipped with a high-temperature heater. However, such a method often cannot provide sufficient dispersibility for nano- and micro-sized agglomerated fillers in high contents.

Ultrasonication followed by suspension blending in ethanol is one of the methods that can be done easily in the lab. The sonication treatment is a form of vibration that generates cavitation or bubbles and provides high intensity of ultrasound energy to the filler [31]. By applying sonication and suspension blending in ethanol, the HA aggregates can be disintegrated and uniformly dispersed in the ethanol suspensions without significant deformation or defects [32]. However, PEEK composite fabrication by suspension blending (SUS) is not convenient either in industrial aspects due to low processability, high production cost, and environmental pollution by the solvents used. Given these conditions, mechanofusion (MF), which is a simple and inexpensive high-throughput compounding system, is an adequate approach to enhance both dispersibility of aggregated filler and compatibility between polymer matrix and filler by high shear and compression forces [33-36]. By MF process, HA particles can be dry-coated onto the surface of PEEK powder, producing a mechanochemical reaction between the host particle, PEEK, and the guest particle, HA [37].

Since the mechanical forces produced by a rotating blade in the chamber break down the fine particle agglomerates, cohesive HA aggregates in PEEK/HA/CF ternary composite can be mechanically dispersed. Moreover, the whole process is cost-effective and environmentally friendly since the MF method can be carried out in dry conditions without any solvents. From the commercial point of view, the manufacturing of PEEK/HA/CF composite at a large scale can be accomplished by using NC-400-P model (Hosokawa Micron), which has a capacity of 10 to 100 kg/hr. To the best of our knowledge, there is no report on the mechanical properties of PEEK/HANF/CF composite prepared by mechanofusion process so far. Hence, this study was conducted to investigate the effect of the non-melt blending process (suspension blending and mechanofusion processing) for PEEK/HA/CF ternary composite on its mechanical properties.

3.2. Materials and Methods

Materials

PEEK powder (Victrex® 450PF) was purchased from Dict Co. (Seoul, Korea). The commercial HA (Nano HAP04) was purchased from Nanjing Emperor Nano Material Co. Ltd. (Nanjing, China). Carbon fiber (PX 35) was obtained from Zoltek (St. Louis, MI, USA). The detailed properties of materials are shown in **Table 3.1**. All the other chemicals were purchased from Sigma-Aldrich Corporation.

Preparation of PEEK composite powders

Two kinds of reinforcements (HA and CF) were blended with the PEEK powder, according to the composition provided in **Table 3.2**. In this study, milled carbon fiber was used instead of short carbon fiber because the bundles of short carbon fiber could not be untangled during the blending process due to weak mechanical force compared to the melt-extrusion method. To prepare composite powders using SUS method, PEEK powder and fillers were separately dispersed in ethanol, followed by ultrasonication for 60 min. Then, each dispersed powder was mixed with another using a magnetic stirrer for 12 hr. The composite suspension was filtered and dried at 110 ℃ for 24 hr.

The equipment for the MF process (Nanocular System, Hosokawa Micron) included a reaction chamber with a rotor that applied strong shear, compressive, and frictional forces to the blended materials [38]. The PEEK, HA, and CF powders were placed in the chamber according to **Table 3.2**. A schematic of the

mechanofusion process to prepare PEEK/HA/CF composite is shown in **Figure 3.1**. Due to the difficulty in the injection process, the maximum amount of the HA and CF fillers was limited to below 40 wt%. To achieve high levels of dispersion through exfoliation of the aggregated HA, the rotor was rotated at 2500 rpm for 1 hr. During the process, the chamber was cooled by circulating water to maintain a constant temperature.

Characterization and measurement of PEEK composites

The surface morphologies of PEEK and CF were characterized by scanning electron microscopy (SEM, Sigma 300, ZEISS). The surface composition of PEEK and CF was determined using energy dispersive spectrometry (EDS), which was coupled with SEM. The fractured surfaces of PEEK/HA/CF composites after flexural testing were also characterized by SEM. The morphology and dispersion state of the HA in the composites were observed by the three-dimensional X-ray micro-computed tomography (micro-CT) (SkyScan 1172, Bruker) [39,40]. The detailed conditions for the micro-CT measurements were as follows. X-ray source voltage and current were 42 kV and 240 μA, respectively. The monitored sample size was 1 × 1 × 1 mm^3. The projection numbers per sample was 1800. The exposure time per projection was 3200 ms. Micro-CT images of the composites were obtained by reconstructing the projections. The size distribution of HA in the composites was investigated using software (CTvox) for three-dimensional modeling.

To evaluate the mechanical properties of PEEK composites, every composite

powder made by both SUS and MF methods was prepared using a mini-injection molding machine (Bautek Co., Uijeongbu-si, Korea) at processing temperatures of 390 ℃. The pre-set molding temperature was set to 190 ℃. The composite powders were molded into 80 × 10 × 4 mm^3 and 10 × 10 × 4 mm^3 plates for flexural and compressive tests, respectively. Then, the composite samples were annealed at 220 ℃ for 4 hr to provide a similar degree of crystallinity.

The flexural and compressive properties were measured with a universal testing machine (Lloyd LR10K, West Sussex, UK) with a load cell of 10 kN, according to the ISO 178 and ISO 604 standards. The cross-head speeds were 2.0 mm/min and 1.0 mm/min for flexural and compression tests, respectively. The average of five measurements was obtained from seven specimens for each test.

3.3. Results and discussion

Morphology of powders

The surface morphologies of PEEK and CF particles in PEEK/HA/CF composite powders prepared by SUS and MF methods are shown in **Figure 3.2**. The surfaces of neat PEEK (**Figure 3.2 (a)**) and CF (**Figure 3.2 (b)**) particles before any treatment exhibited smooth and clean surfaces. As shown in **Figure 3.2 (c)**, HA aggregates were adhered to the surface of PEEK particles, but not the surface of CF. On the other hand, the surfaces of both PEEK and CF were covered with HA fillers after MF process (**Figure 3.2 (d)**). The attached HA particles were confirmed by EDS mapping of Ca. The MF processing could induce the mechanical interlocking at the interface of different components by applying strong mechanical forces [41,42]. PEEK/HA/CF composite fabricated using HA-covered PEEK and CF was expected to show improved interfacial adhesion between PEEK matrix and fillers. Furthermore, molten PEEK during the injection molding process was expected to penetrate the microgaps formed between HA particles on the CF surface, resulting in improved interfacial strength through mechanical interlocking between components [43].

Mechanical properties

The results of flexural strength test are shown in **Table 3.3**. Composite samples prepared by both SUS and MF method showed an increase in flexural strengths and modulus as the CF content increased. The flexural strengths of C1, C2, and C3 made by MF process were 185, 221, and 254 MPa, respectively. Compared to C1,

C2, and C3 samples made by the SUS method, mechanofused samples showed similar values in the flexural strengths within the error range. The applied mechanical forces by MF process were not effective on the micro-sized CF fillers compared to the nano-sized HA fillers that are easily aggregated. Due to the high modulus and stiffness characteristics of the CF filler [44], the flexural moduli for samples prepared by both methods were increased as with increasing CF content. In contrast, the flexural strains at the break decreased with an increasing CF content due to the rigid characteristics of CF filler, resulting in fracture-behavior transition from ductile to brittle.

When the HA filler was added to the composite, both flexural strength and strain at break were decreased regardless of methods as shown in **Figure 3.3**. With the SUS method, the flexural strengths of H1C1 and H2C1 composites were decreased 9.3% and 27.4%, respectively, from 182 MPa of C1 sample. This reduction in strength was mainly due to a strong HA agglomeration, causing the growth of microcracks from applied external forces. However, the flexural strengths of H1C1 and H2C1 composites prepared by MF process were only decreased 3.8% and 7.0%, respectively, implying that the MF process was able to well pulverize HA aggregates and enhance HA dispersibility in the polymer matrix. Thus, the HA reinforced composites prepared by the MF method showed much improved flexural strength compared to the ones prepared by the SUS method, particularly H2C1 sample, which improved 30%. Compared to the flexural strength values of cortical bone that ranged from 103 to 238 MPa [45], the flexural strength of H2C1 composite was found to match the middle range. This could be further increased with the addition of CF filler. The strain to failure value of H2C1 composite

prepared by the MF method was closely matched to the value of cortical bone that ranged from 1 to 3% [46]. As shown in **Figure 3.4**, the flexural modulus of PEEK composites from both SUS and MF methods increased as HA content was increased. The lamellar microcrystals between the PEEK matrix and the HA nanoparticles increased the modulus of elasticity by reducing the elastic resistance [29].

Table 3.3 showed the compressive strength data of PEEK composites. Similar to the flexural properties in C1, C2, and C3 samples, the compressive strength and modulus were also increased with the addition of CF filler. However, there was no significant change in the flexural properties between the C1, C2, and C3 composites prepared by SUS or MF method. After the incorporation of the HA filler, the compressive strength was improved by both methods as shown in **Figure 3.5**. Among various bioactive ceramics, HA, which has low porosity and dense structure, could increase compressive strength with increasing content [47]. The composites prepared by the MF method showed higher compressive strength than the ones prepared by the SUS method because of the enhanced pulverization and dispersibility of the HA nanofiller. The compressive strength of H2C1 sample made by the MF method found to be in the middle range of cortical bone (e.g. 106 to 215 MPa) [48] and could be further improved with the addition of CF filler.

Morphology of composites

3D X-ray micro-CT analysis is a non-destructive investigation method used to precisely examine the internal structure of polymer composites [49,50]. **Figure 3.6** showed the dispersion of the HA filler in H2C1 composite by using the 3D X-ray

micro-CT. The observed dimensions of the composites were 0.5 × 0.5 × 0.5 mm^3. The average size of the HA filler in H2C1 composite by the SUS method (**Figure 3.6 (a)**) was larger than 100 μm, indicating a strong aggregation of HA particles. Moreover, a number of the HA aggregates that are larger than 400 μm were observed. In contrast, the average size of the HA filler by the MF method was less than 20 μm, implying small aggregations since the original average size of HA in the technical specification was about 150 nm. HA was better dispersed by the MF method (**Figure 3.6 (b)**) than by the SUS method due to enhanced shear, compressive, and frictional forces. It can be concluded that the strong mechanical forces during MF process could enhance the dispersibility of HA filler, thereby improving both flexural and compressive strength of the PEEK/HA/CF ternary composite.

The fractured sections of H2C1 composite after flexural testing were observed to investigate the dispersibility of the HA filler. As shown in **Figure 3.7**, the fracture morphologies of both composites were changed from ductile to brittle failure due to HA and CF fillers. It can be seen that the main fracture mechanism occurred by aggregation of HA fillers. It was important to note that severely aggregated HA fillers were easily observed in the H2C1 composite made by the SUS method (**Figure 3.7 (a)**), whereas the HA fillers in the H2C1 composite made by the MF method were dispersed better with a size of about 1 μm (**Figure 3.7 (b)**). The poor interfacial interaction between HA and PEEK matrix was another reason for early failure of composites. In both H2C1 composites, the majority of the HA particles showed adhesive failure due to interfacial de-bonding with the PEEK matrix.

In the case of micro-sized CF filler, PEEK/HA/CF composite fabricated using

HA covered PEEK and CF exhibited improved interfacial adhesion via the entanglement of interfacial HA particles, acting as a bridging material between PEEK and CF. The improved strength of the interfacial adhesion between PEEK matrix and CF fillers indicated the stresses applied to the composites were transferred from the PEEK matrix to the CF fillers, resulting in improved mechanical strengths of PEEK/HA/CF composite prepared by the MF method. These results demonstrated that MF method could improve flexural and compressive strengths of PEEK/HA/CF ternary composite by enhancing dispersion of the HA aggregates and interfacial adhesion between matrix and fillers.

3.4. Conclusion

Comparison in mechanical properties of PEEK/HA/CF ternary composite fabricated through SUS and MF methods revealed that composite from the latter method had better properties. Higher flexural and compressive strengths and elongation at break were achieved through MF technique as compared to dispersion in ethanol. Improvements in dispersibility of the HA particles and interfacial adhesion between components were seen through 3D X-ray micro-CT and SEM micrographs, indicating a good blending of fillers with the polymer matrix. The H2C1 composite made by the MF method was found to match the middle range of cortical bone in both flexural and compressive strength. The results demonstrated MF method as a better fabrication process for producing PEEK/HA/CF ternary composite compared to ethanol mixing, with the advantages of solvent-free, better processability, and cost-effectiveness.

Table 3.1. Properties of materials.

	PEEK	HA	CF
Product name	Victrex 450PF	Nano HAP04	PX 35
Diameter / Length	50 μm	20 nm / 150 nm	7.2 μm / 150 μm
Tensile strength	98 MPa	-	4137 MPa
Tensile modulus	4 GPa	-	242 GPa
Flexural strength	165 MPa	-	-
Flexural modulus	3.8 GPa	-	-
Compressive strength	125 MPa	-	-
Density	1.3 g/cm^3	-	1.81 g/cm^3

Table 3.2. Formulation ratios of the PEEK composites.

Sample code	PEEK content (wt%)	HA content (wt%)	CF content (wt%)
PEEK	100	0	0
C1	90	0	10
C2	80	0	20
C3	70	0	30
H1C1	80	10	10
H1C2	70	10	20
H1C3	60	10	30
H2C1	70	20	10
H2C2	60	20	20

Table 3.3. Mechanical properties of PEEK composites.

	Flexural Modulus (GPa)		Flexural Strength (MPa)		Flexural Strain at Break (%)		Compressive Modulus (GPa)		Compressive Strength (MPa)	
	SUS	MF	SUS	MF	SUS	MF	SUS	MF	SUS	MF
PEEK	3.7 ± 0.2		155 ± 3		-		2.7 ± 0.1		120 ± 2	
C1	5.6 ± 0.1	5.7 ± 0.3	182 ± 3	185 ± 3	5.5 ± 0.3	5.4 ± 0.2	3.5 ± 0.1	3.6 ± 0.1	134 ± 1	135 ± 3
C2	8.7 ± 0.2	8.9 ± 0.3	219 ± 2	221 ± 2	3.8 ± 0.3	3.9 ± 0.1	4.0 ± 0.1	3.9 ± 0.1	151 ± 3	153 ± 4
C3	13.5 ± 0.4	13.5 ± 0.4	252 ± 5	254 ± 4	2.5 ± 0.1	2.4 ± 0.1	4.5 ± 0.1	4.4 ± 0.1	168 ± 2	170 ± 3
H1C1	7.7 ± 0.1	7.3 ± 0.1	165 ± 4	178 ± 1	2.4 ± 0.1	4.0 ± 0.1	2.3 ± 0.1	2.4 ± 0.1	139 ± 2	149 ± 2
H1C2	11.0 ± 0.2	10.9 ± 0.2	198 ± 3	215 ± 1	2.1 ± 0.1	3.2 ± 0.1	4.1 ± 0.2	2.6 ± 0.1	158 ± 2	170 ± 3
H1C3	18.2 ± 0.9	17.7 ± 0.3	228 ± 7	246 ± 2	1.5 ± 0.1	1.9 ± 0.1	4.6 ± 0.3	3.2 ± 0.2	178 ± 2	198 ± 3
H2C1	8.8 ± 0.1	8.9 ± 0.4	132 ± 3	172 ± 2	1.6 ± 0.1	2.4 ± 0.1	3.8 ± 0.1	3.2 ± 0.2	151 ± 5	167 ± 3
H2C2	13.3 ± 0.2	13.5 ± 0.1	163 ± 13	206 ± 3	1.4 ± 0.1	1.8 ± 0.1	4.5 ± 0.1	3.4 ± 0.1	170 ± 6	192 ± 3

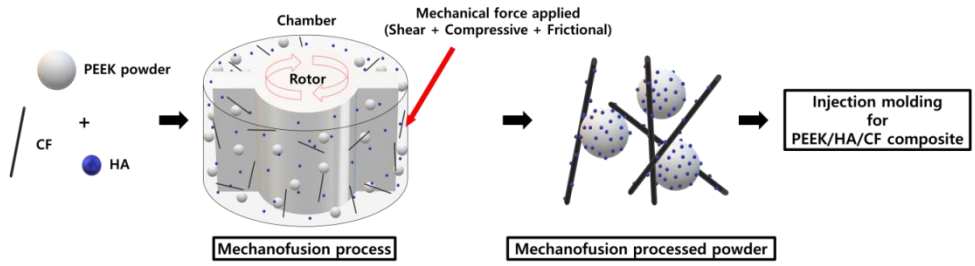

Figure 3.1. A schematic of mechanofusion process to prepare PEEK/HA/CF composite.

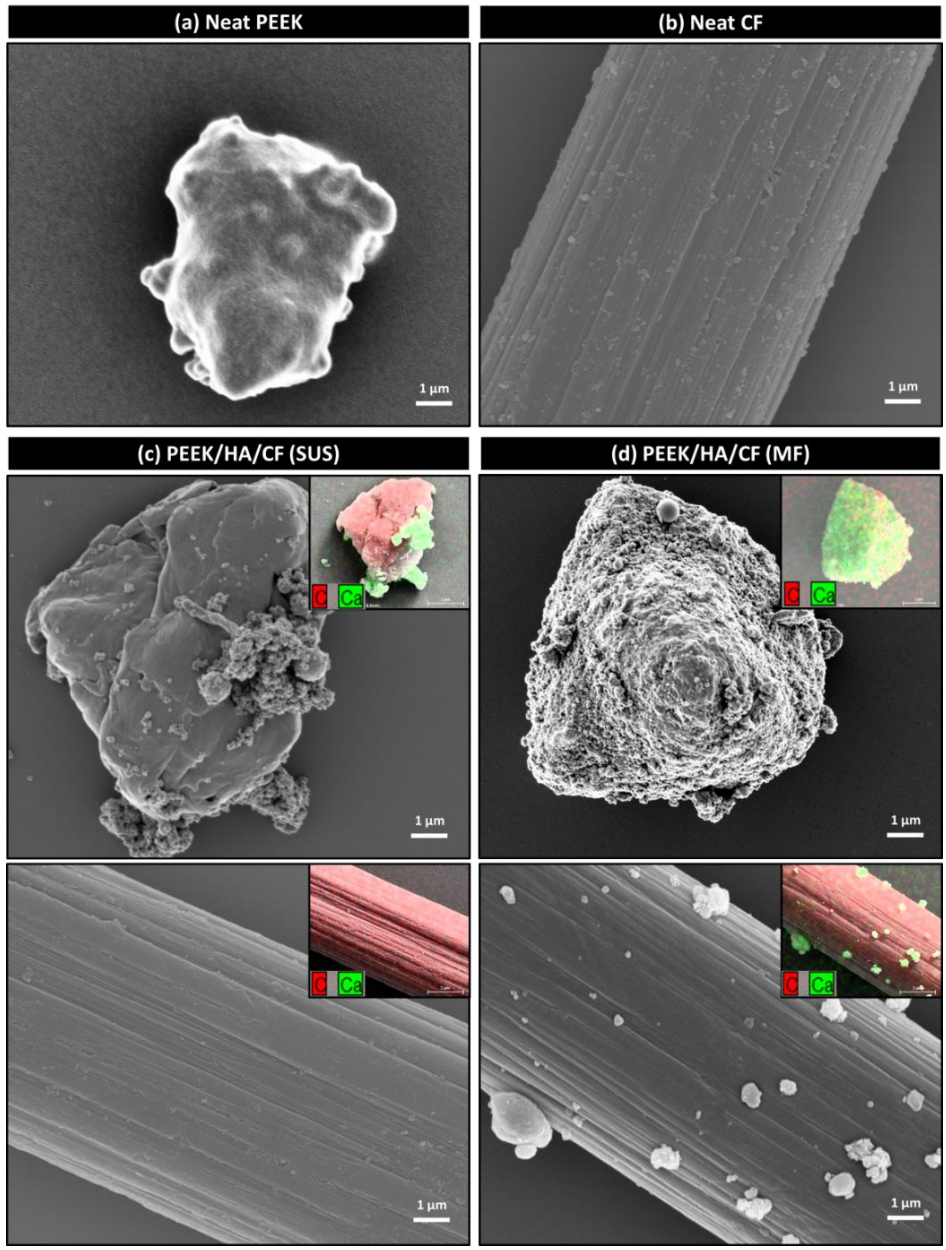

Figure 3.2. SEM images of (a) PEEK and (b) CF surfaces; SEM images and corresponding EDS mapping of C and Ca for PEEK/HA/CF composite powder on PEEK and CF surfaces prepared by (c) SUS and (d) MF methods.

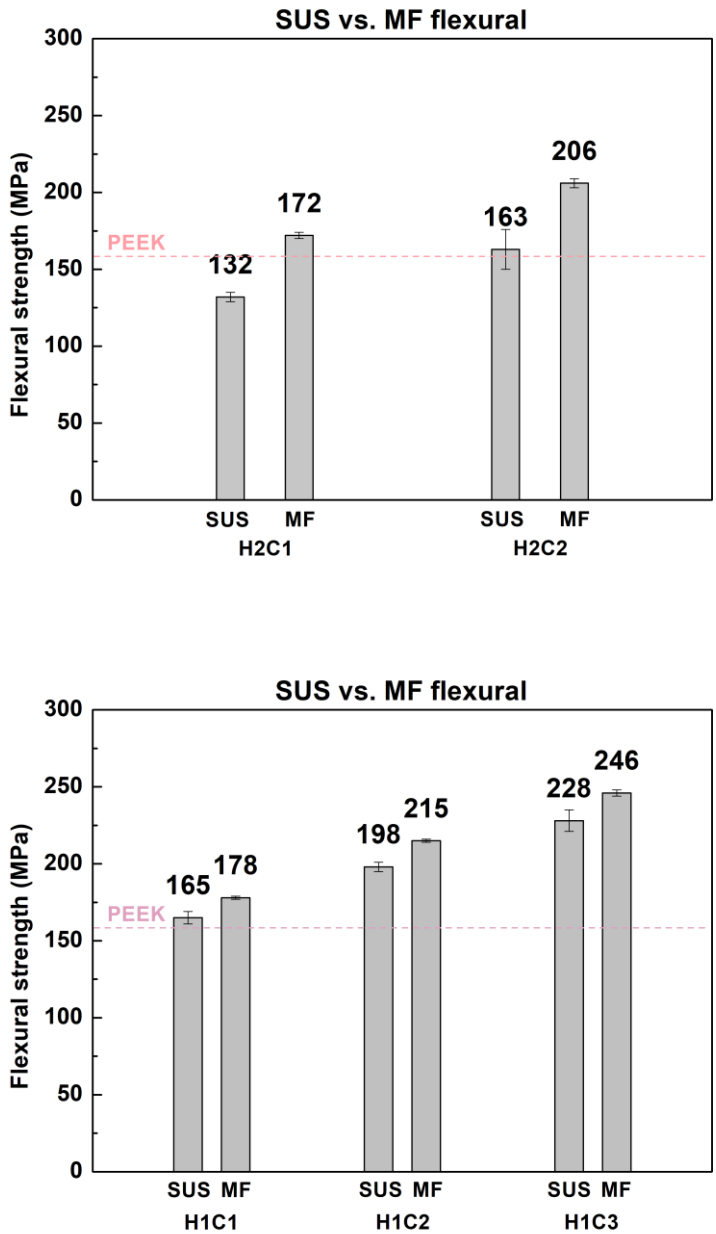

Figure 3.3. Flexural strength of PEEK/HA/CF composites prepared by SUS and MF methods.

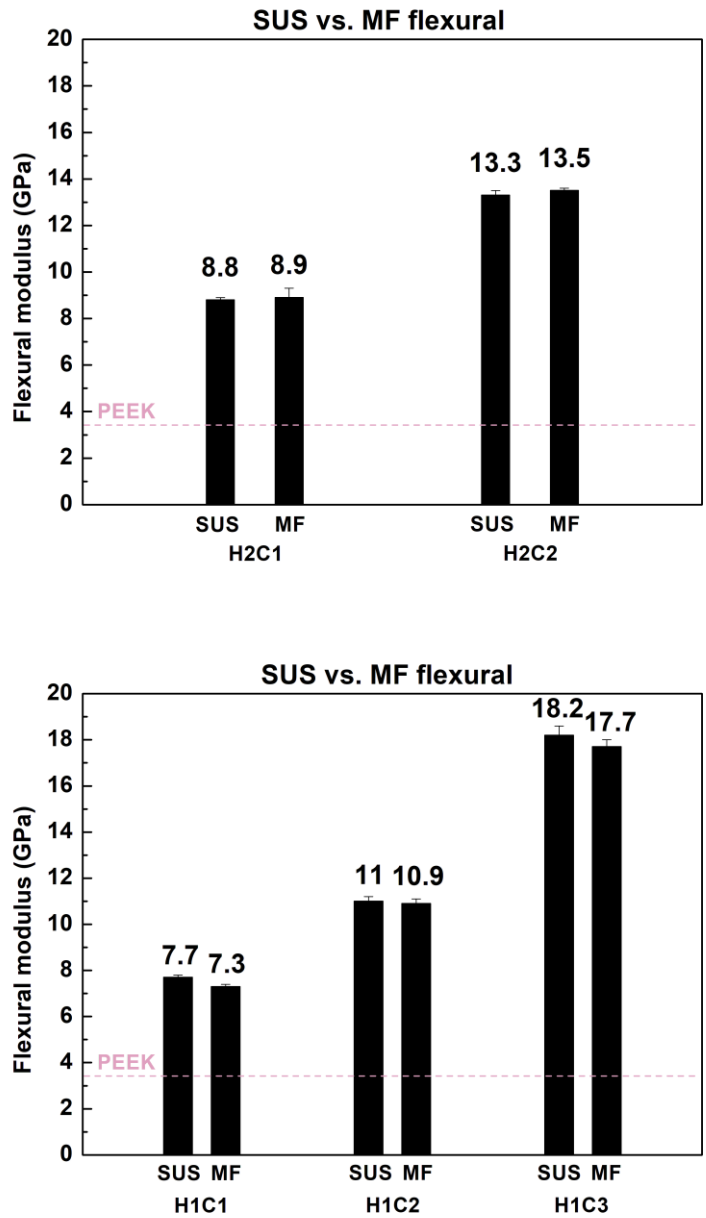

Figure 3.4. Flexural modulus of PEEK/HA/CF composites prepared by SUS and MF methods.

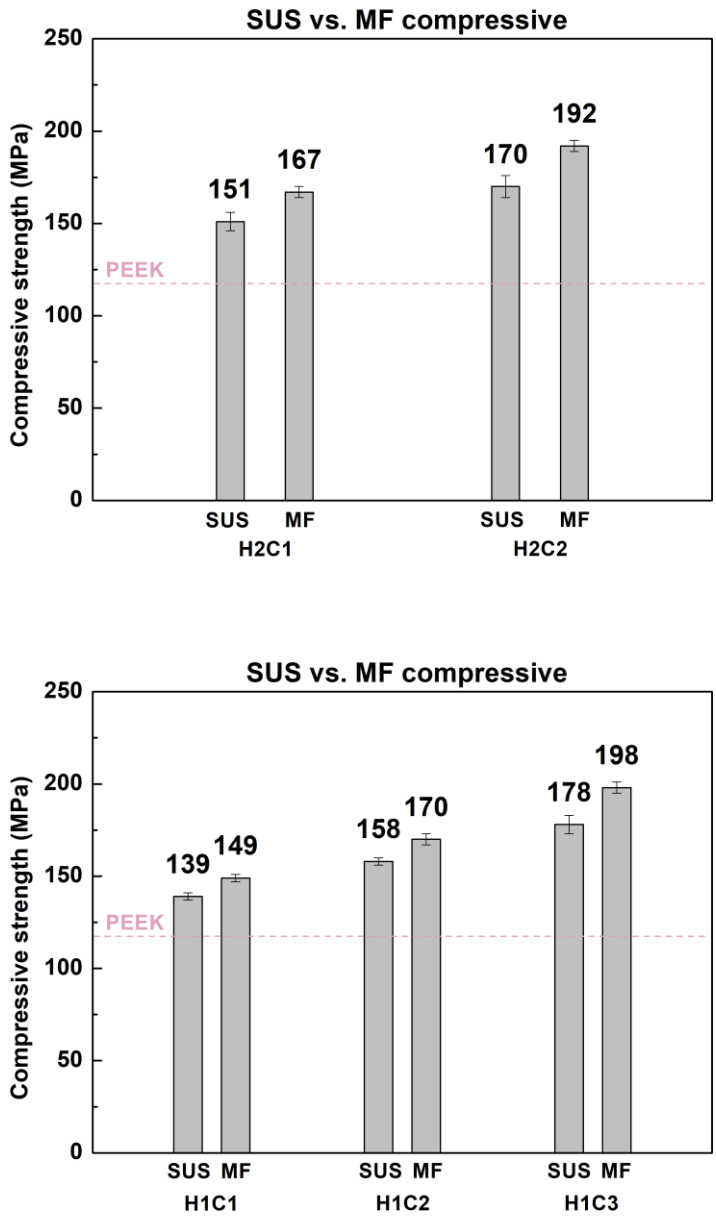

Figure 3.5. Compressive strength of PEEK/HA/CF composites prepared by SUS and MF methods.

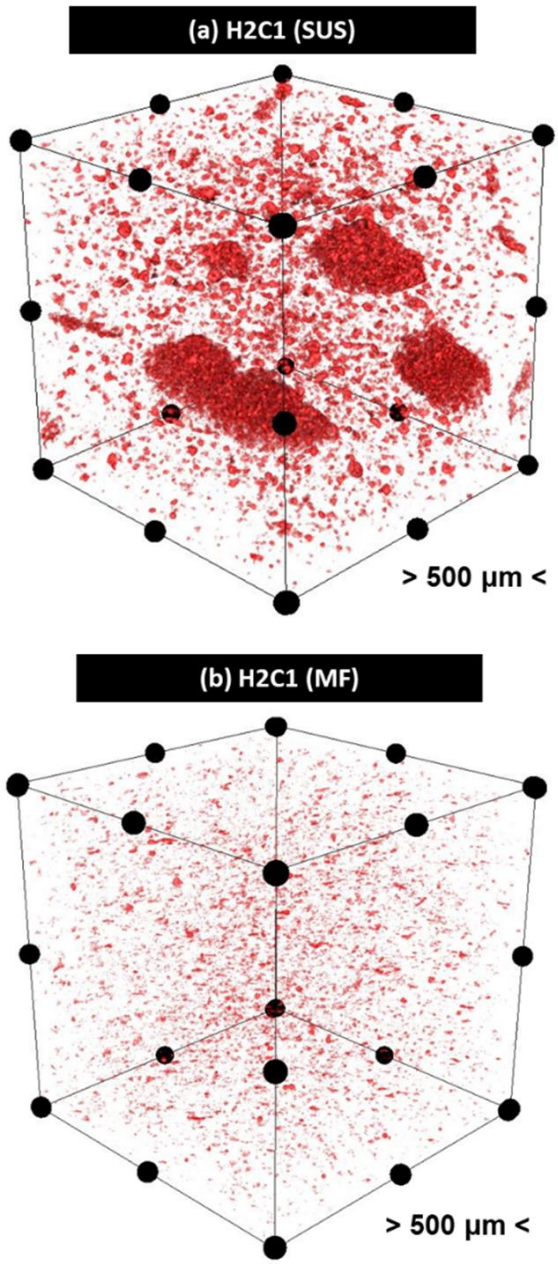

Figure 3.6. Three-dimensional X-ray micro-CT analysis on H2C1 composites prepared by (a) SUS and (b) MF methods.

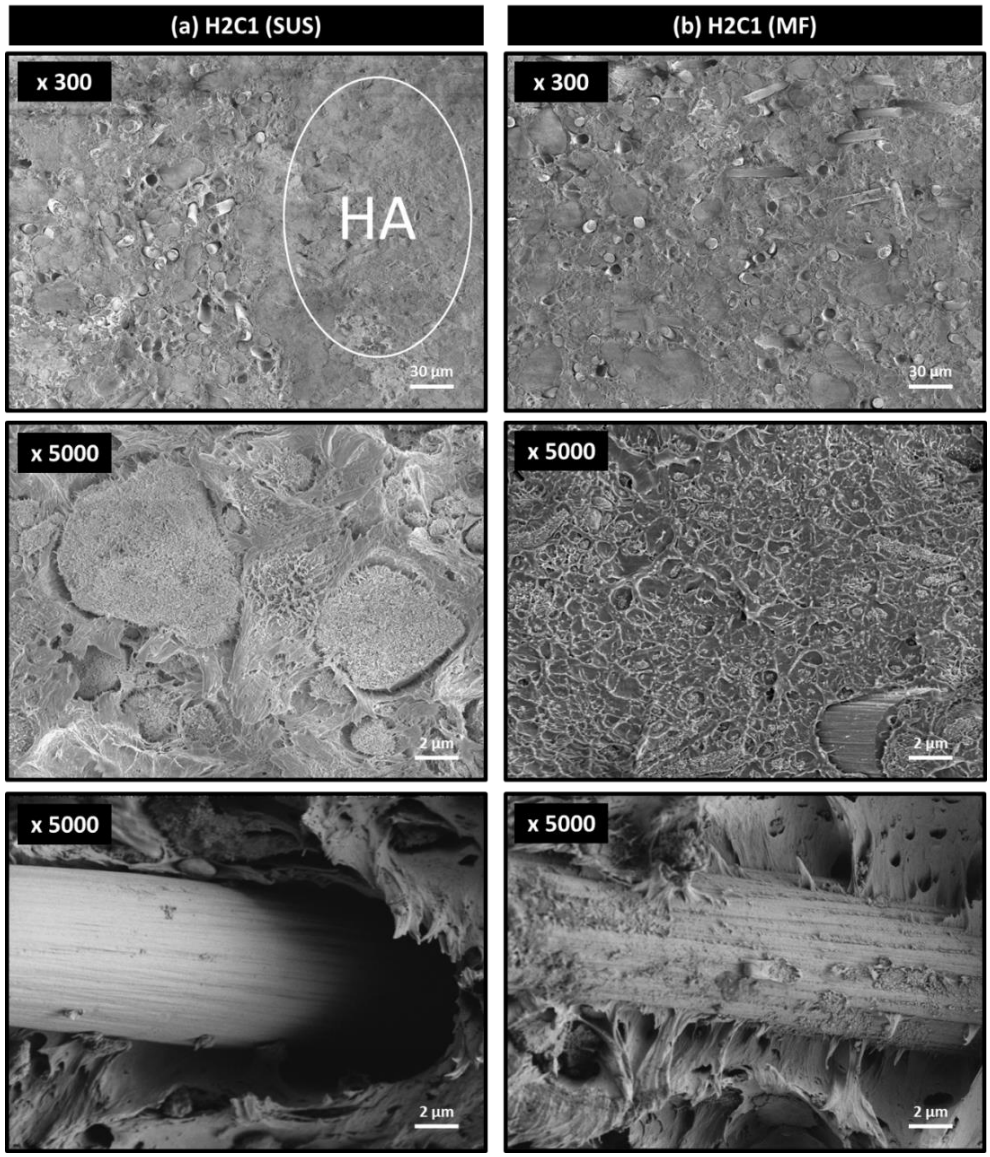

Figure 3.7. Fracture morphologies of H2C1 composites prepared by (a) SUS and (b) MF methods.

3.5. References

[1] A. Warburton, S. J. Girdler, C. M. Mikhail, A. Ahn, S. K. Cho, *Neurospine*, **2020**, *17*, 101.

[2] L. Wang, S. He, X. Wu, S. Liang, Z. Mu, J. Wei, F. Deng, Y. Deng, S. Wei, *Biomaterials*, **2014**, *35*, 6758.

[3] K. Goto, Y. Kuroda, T. Kawai, K. Kawanabe, S. Matsuda, *Bone Joint J.*, **2019**, *101*, 787.

[4] Đ. Vukajlović, O. Bretcanu, K. Novakovic, *You-CGMed-Workshop for Young Researchers in Ceramics and Glasses for Medical Applications, Newcastle University* **2019**.

[5] S. Ramakrishna, J. Mayer, E. Wintermantel, K. W. Leong, *Compos. Sci. Technol.*, **2001**, *61*, 1189.

[6] S. M. Kurtz, J. N. Devine, *Biomaterials*, **2007**, *28*, 4845.

[7] J. M. Toth, M. Wang, B. T. Estes, J. L. Scifert, H. B. Seim III, A. S. Turner, *Biomaterials* **2006**, *27*, 324.

[8] L. Cheng, L. Nie, L. Zhang, *Int. Orthopaed.*, **2009**, *33*, 1043.

[9] A. H. Glassman, J. D. Bobyn, M. Tanzer, *Clin. Orthop. Relat. Res.*, **2006**, *453*, 64.

[10] C. K. Seal, K. Vince, M. A. Hodgson, *IOP Conf. Ser. Mater. Sci. Eng.*, **2009**, *4*, 012011.

[11] M. Niinomi, *Mater. Sci. Eng. A*, **1998**, *243*, 231.

[12] J. Y. Rho, R. B. Ashman, C. H. Turner, *J Biomech.*, **1993**, *26*, 111.

[13] J. Sandler, P. Werner, M. S. Shaffer, V. Demchuk, V. Altstädt, A. H. Windle, *Compos. Part A: Appl. Sci. Manuf.*, **2002**, *33*, 1033.

[14] M. -C. Hung, S. -Y. Yuan, S. I. Chang, J. -W. Liao, T. -H. Ko, C. -L. Cheng, *Carbon*, **2014**, *68*, 628.

[15] A. Saleem, L. Frormann, A. Iqbal, *Polym. Compos.*, **2007**, *28*, 785.

[16] C. S. Li, C. Vannabouathong, S. Sprague, M. Bhandari, *Clinical Medicine Insights: Arthritis and Musculoskeletal Disorders*, **2015**, *8*, 33.

[17] Y. Deng, P. Zhou, X. Liu, L. Wang, X. Xiong, Z. Tang, J. Wei, S. Wei, *Colloids Surf. B Biointerfaces*, **2015**, *136*, 64.

[18] Y. Hwang, M. Kim, J. Kim, *Compos. Part A Appl. Sci. Manuf.*, **2013**, *55*, 195.

[19] H. J. Song, N. Li, Y. Li, C. Min, Z. Wang, *J. Mater. Sci.*, **2012**, *47*, 6436.

[20] J. A. Puértolas, M. Castro, J. A. Morris, A. Ríos, A. Ansón-Casaos, *Carbon*, **2019**, *141*, 107.

[21] R. Ma, S. Tang, H. Tan, J. Qian, W. Lin, Y. Wang, C. Liu, J. Wei, T. Tang, *ACS Appl. Mater. Interfaces*, **2014**, *6*, 12214.

[22] R. K. Roeder, G. L. Converse, R. J. Kane, W. Yue, *JOM*, **2008**, *60*, 38

[23] C. H. Hammerle, A. J. Olah, J. Schmid, L. Fluckiger, S. Gogolewski, J. R. Winkler, N. P. Lang, *Clin. Oral Implants Res.*, **1997**, *8*, 198.

[24] T. J. Webster, C. Ergun, R. H. Doremus, R. W. Siegel, R. Bizios, *Biomaterials*, **2000**, *21*, 1803.

[25] M. A. Abu Bakar, P. Cheang, K. A. Khor, *Comp. Sci. Tech.*, **2003**, *63*, 421.

[26] P. R. Monich, B. Henriques, A. P. N. de Oliveira, J. C. M. Souza, M. C. Fredel, *Mat. Lett.*, **2016**, *185*, 593.

[27] L. M. Mathieu, P. -E. Bourban, J. -A. E. Månson, *Compos. Sci. Technol.*, **2006**, *66*, 1606.

[28] M. S. Abu Bakar, P. Cheang, K. A. Khor, *Mater. Sci. Eng. A*, **2003**, *345*, 55.

[29] R. Ma, Q. Li, L. Wang, X. Zhang, L. Fang, Z. Luo, B. Xue, L. Ma, *Mater. Sci. Eng. C Mater. Biol. Appl*, **2017**, *73*, 429.

[30] X. Feng, G. Sui, R. Yang, Chin. *J. Mater. Res.*, **2008**, *22*, 18.

[31] I. Kaur, L. J. Ellis, I. Romer, R. Tantra, M. Carriere, S. Allard, M. Mayne-L'Hermite, C. Minelli, W. Unger, A. Potthoff, S. Rades, E. Valsami-Jones, *J. Vis. Exp.*, **2017**, *130*, e56074.

[32] T. Peng, I. Chang, *Powder Technol.*, **2015**, *284*, 32.

[33] Y. M. Lee, J. You, M. Kim, T. A. Kim, S. -S. Lee, J. Bang, J. H. Park, *Compos. B Eng.*, **2019**, *165*, 725.

[34] M. Alonso, F. J. Alguacil, *Rev. Metal.*, **1999**, *35*, 315

[35] T. Yokoyama, C. C. Huang, *KONA*, **2005**, *23*, 7.

[36] J. Koskela, D. A. V. Morton, P. J. Stewart, A. M. Juppo, S. Lakio, *Int. J. Pharm*., **2018**, *537*, 64.

[37] O. Y. Posudievsky, O. A. Kozarenko, V. S. Dyadyun, S. W. Jorgensen, J. A. Spearot, V. G. Koshechko, V. D. Pokhodenko, *J. Power Sources*, **2011**, *196*, 3331.

[38] J. You, H. -H. Choi, J. Cho, J. G. Son, M. Park, S. -S. Lee, J. H. Park, *Compos. Sci. Technol*., **2018**, *160*, 245.

[39] H. S. Kim, H. S. Bae, J. Yu, S. Y. Kim, *Sci. Rep*., **2016**, *6*, 26825.

[40] H. S. Kim, J. H. Kim, W. Y. Kim, H. S. Lee, S. Y. Kim, M. -S. Khil, *Carbon*, **2017**, *119*, 40.

[41] R. Pfeffer, R. N. Dave, D. Wei, M. Ramlakhan, *Powder Technol*., **2001**, *117*, 40.

[42] Q. T. Zhou, L. Qu, I. Larson, P. J. Stewart, D. A. V. Morton, *Powder Technol*., **2011**, *207*, 414.

[43] J. Jang, H. Yang, *J Mater. Sci*., **2000**, *35*, 2297.

[44] P. Bhatt, A. Goel, *Mater. Sci. Res. India*, **2017**, *14*, 52.

[45] J. R. Caeiro, P. González, D. Guede, *Rev. Osteoporos. Metab. Miner.*, **2013**, *5*, 99.

[46] M. Wang, D. Porter, W. Bonfield, *Br. Ceram. Trans*., **1994**, *93*, 91.

[47] M. Prakasam, J. Locs, K. Salma-Ancane, D. Loca, A. Largeteau, L. Berzina-Cimdina, *J. Funct. Biomater*., **2015**, *6*, 1099.

[48] A. C. Lawson, J. T. Czernuszka, *Proc. Instn. Mech. Engrs.-Part H*, **1998**, *212*, 413.

[49] J. You, H. -H. Choi, Y. M. Lee, J. Cho, M. Park, S. -S. Lee, J. H. Park, *Compos. B*, **2019**, *164*, 710.

[50] J. You, H. -H. Choi, T. A. Kim, M. Park, J. S. Ha, S. -S. Lee, J. H. Park, *Compos. Sci. Technol*., **2019**, *183*, 107800d.

Chapter 4

Mechanical Strength of Polyetheretherketone Copolymer Composite Reinforced with Graphene Oxide and Carbon Fiber

The results described in this part have been published in *Polymers. 2019 November 11(11): 1803*

4.1. Introduction

The spine plays two important and distinct roles. It provides a strong central axis for the appendicular skeleton and protects the spinal cord and the roots of delicate nerves connect to the brain. Therefore, the artificial bone graft materials used in the spine cage development must have proper strength and stiffness as well as the capability to bond to vertebrae. Metallic materials, such as titanium alloy and stainless steel, have been commonly used in spine cages with competent mechanical properties and biologically inert properties [1,2]. Despite the outstanding benefits of metallic materials for spine cage application, several concerns have been raised due to the stress shielding effect, low biocompatibility, release of ionic effluence, magnetic image interference, and additional second surgery required for removal. Typically, the Young`s modulus of these alloys (titanium alloy 80 to 125 GPa and magnesium alloy 41 to 45 GPa) is shown too high than that of the human bone (~14 GPa). The mismatch of the Young`s moduli between metallic materials and the human bone could induce a stress shielding effect on the bone [3], which can lead implant loosening, bone thickening, and chronic inflammation [4].

To overcome the several concerns associated with the use of metallic materials, polyaryletherketones (PAEKs), including the polyetheretherketone (PEEK) group, have been employed as biomaterials for spine cages [5]. PEEK polymers have specific thermal processing condition due to their crystal structures [6]. Therefore, a copolymerization method between various PEEKs was applied to fit the mechanical properties of PEEK polymers [7]. PEEK polymers find applications as

high performance super engineering plastics. However, due to its high glass transition temperature (T_g) and high melting point (T_m) [8,9] the processing temperature of PEEK is very high. Several modifications were reported in order to reduce the processing temperature, such as lowering the T_m and softening the backbone of the PEEK [10-12]. In the present paper, P(E2-E4)K, composed of "-ether-phenyl-ether-phenyl-ether-phenyl-ether", was used as matrix polymer. The four ether groups (E4: EEEE) could greatly affect the distribution of the flexible and rigid segments on their molecule chains.

Regarding the mechanical strength of cortical bone, the flexural and compressive strength of human cortical bone have been reported in the range of 103 to 238 and 130 to 213 MPa, respectively [13,14]. Since the mechanical strength of PEEK is in the low range, PEEK should be further reinforced to fit in the high range in order to be applied for various patients. One of carbon fillers that is commonly used as reinforcement for the spine cages is carbon fiber (CF) because of its high mechanical property, thermal resistance, wearability, and biocompatibility [15,16]. Another carbon filler that can be used is graphene oxide (GO), a promising filler for both mechanical and biological applications due to its high surface area and hydrophilic oxygen-rich functional groups on the surface [17]. Several studies show that the mechanical properties of various polymers were enhanced by adding GO but decreased after adding 1 wt% of GO or more due to the aggregation of GO nanosheets [18-20]. According to recent studies, low concentration of GO has been confirmed to be non-toxic and biocompatible because of the oxygen-rich functional groups which enhance cell adhesion and spreading [21-23]. In this study, PEEK/GO composite was prepared and tested for the flexural strength to confirm

the appropriate content of GO for P(E2-E4)K/GO/CF composite. Then, we evaluated the flexural and compressive strengths of P(E2-E4)K composite.

4.2. Materials and Methods

Materials

P(E2-E4)K copolymer was kindly provided by the Nanobiomaterial Lab., Dept. of Polymer Science and Engineering of Sungkyunkwan University (Suwon, Korea). PEEK powder (Victrex® 450PF) was purchased from Dict Co. (Seoul, Korea). Graphene oxide powder (purity >99 wt%, lateral dimension ≥7 μm, thickness 1.1 to 1.3 nm) was purchased from LS-Chem (Ochang, Korea). Milled carbon fiber (PX35, average length 150 μm, average diameter 7.2 μm) was purchased from Zoltek Co. (Missouri, USA).

Preparation of PEEK and P(E2-E4)K composites

To prepare blend powders, PEEK or P(E2-E4)K powder was dispersed in a beaker containing ethanol, followed by ultrasonication for 30 min. The dispersion of GO and CF fillers was also separately prepared in same way. Subsequently, each dispersed powder sample was mixed with another using a magnetic stirrer for 12 hr, according to the composition provided in **Table 4.1**. The composite suspension was filtered and vacuum-dried at 60 ℃ for 24 hr. Milled carbon fiber was used instead of short carbon fiber because the bundles of short carbon fiber could not be untangled with suspension blending method due to weak mechanical force compared to the melt-extrusion method.

For evaluation of flexural and compressive strengths, the blended powder samples were molded using a mini-injection molding machine (Bautek Co., Uijeongbu-si, Korea) at processing temperatures of 390 ℃, with a pre-set molding

temperature at 190 ℃. A flexural test specimen of 80 × 10 × 4 mm^3 and compression test specimen of 10 × 10 × 4 mm^3 were prepared using the above procedure. To ensure a similar degree of crystallinity, all the samples were annealed at 220 ℃ for 4 hr.

Characterization and measurement of PEEK and P(E2-E4)K composites

The flexural strength and compressive strength were measured according to the ISO 178 and ISO 604 standards, respectively. A Universal Test Machine (Lloyd LR10K, West Sussex, UK) with a load cell of 10 kN was used for the test. The cross-head speeds were 2.0 mm/min and 1.0 mm/min for flexural and compression testing, respectively. The average of five measurements was obtained from seven specimens for each test. The fracture surface of composites after flexural testing was characterized by scanning electron microscopy (SEM, Sigma 300, ZEISS).

4.3. Results and discussion

PEEK/GO composite

The flexural strength test results were shown in **Table 4.2**. The flexural strengths for Samples No. 1, No. 2, and No. 3 were 154, 161, and 156 MPa, respectively. The relationship between flexural stress and strain in the composite samples was demonstrated in **Figure 4.1**. Compared with the neat PEEK, No. 1 sample, the flexural strength of No. 2 sample was slightly increased by 4.5%. This was due to the hydrogen bonding and π-π stacking interaction. GO nanosheets, containing hydroxyl and carboxylic groups on the surface, could interact with carbonyl groups in PEEK matrix through hydrogen bonding. Moreover, the interfacial adhesion between GO and PEEK matrix could be enhanced through π-π stacking interaction due to the conjugated structure of GO and the benzene rings of PEEK. When the content of GO was further increased to 1 wt% in No. 3 sample, both the flexural strength and the elongation at break were decreased. This result was similar with other GO reinforced polymer composites [24-26]. This reduction with increasing GO content could be due to the aggregation of GO nanosheets that can initiate the micro-sized cracks and decrease the yield strength as a result. As shown in **Figure 4.2**, the thickness of GO was drastically increased for No. 3 sample compared to No. 2 sample. The addition of GO content over 0.5 wt% led to the aggregation of GO nanosheets, which could be found in voids on the fracture surfaces. Thereby, the flexural strength of PEEK/GO composite could be optimized at the GO content of 0.5 wt%.

P(E2-E4)K/GO/CF composite

The flexural and compressive strength test results of P(E2-E4)K composites were shown in **Table 4.3**. The flexural strengths for the samples No. 4, No. 5, and No. 6 were 155, 240, and 250 MPa, respectively. The relationship between the flexural stress and strain in the composite samples was demonstrated in **Figure 4.3**. The flexural properties of No. 2 and No. 3 exhibited higher yield stress and modulus but lower break energy compared to those of No. 1. The flexural strength of No. 2 and No. 3 were enhanced by 54.8% and 61.3%, respectively compared to that of No. 1 due to the high stiffness and modulus characteristics of the CFs [27]. The addition of GO increased the flexural strength by 10 MPa from No. 2 sample since GO played a role in load transfer through strong interaction with copolymer matrix.

The incorporation of GO improved the mechanical strength through two mechanisms: formation of π-π stacking interaction between the conjugated structure of GO and the benzene rings of copolymer, and hydrogen bonding between hydroxyl and carboxylic groups of GO and carbonyl group in the matrix [28,29]. The composite samples generally showed a sharp drop in strain after 2.8% due to the rigid characteristics of CF and GO fillers. This suggested a shift from ductile to brittle fracture behavior. As shown in **Figure 4.4 (a)**, No. 1 sample showed smooth surface in conjunction with river patterns, indicating a typical ductile fracture behavior. When GO and CFs were added (**Figure 4.4 (b)** and **4.4 (c)**), the fracture surface became much rougher with multilayer structure due to many interface debonding and pullout of CFs. Most of CFs in both No. 2 and No. 3 showed a smooth surface with little copolymer attached, indicating a weak

interfacial adhesion between CF and copolymer matrix. This could be the main reason for the failure mode.

The compressive strengths for No. 1, No. 2, and No. 3 in MPa were 125, 161, and 164, respectively, as shown in **Table 4.3**. Compared to the compressive strength of No. 1, those of No. 2 and No. 3 exhibited a sharp increase by 28.9% and 31.2%, respectively. As shown in **Figure 4.5**, the carbon fillers not only increased both yield strength and modulus but also reduced break energy similar to the flexural strength test results. Furthermore, the compressive strength was slightly increased by 1.8% with the addition of GO. However, the improved compressive strength was primarily governed by the mechanical properties of the CFs rather than the properties of GO.

4.4. Conclusion

In this study, the flexural and compressive strength of P(E2-E4)K copolymer composite reinforced with GO and CF were investigated for use in spine cages as a prosthetic. Based on the flexural strength test of PEEK/GO composite, the optimized content of GO was found to be 0.5 wt%. When the GO content exceeded 0.5 wt%, the aggregation of GO nanosheets became severe, resulting in a decrease in mechanical properties. In case of P(E2-E4)K copolymer composites, both flexural and compressive strengths were enhanced by incorporation of 0.5 wt% GO and 30 wt% CF. It was confirmed that P(E2-E4)K/GO/CF composite prepared in this study had adequate mechanical strengths to be used as an implant material for spinal fixation.

Table 4.1. Formulation ratios of the PEEK and P(E2-E4)K composites.

Sample Name	Sample content (wt%)
No. 1	PEEK only
No. 2	PEEK / GO(0.5)
No. 3	PEEK / GO(1)
No. 4	P(E2-E4)K only
No. 5	P(E2-E4)K / CF(30)
No. 6	P(E2-E4)K / GO(0.5) / CF(30)

Table 4.2. Flexural strength test result of the PEEK/GO composites.

Sample Name	Sample content (wt%)	Flexural strength (MPa)
No. 1	PEEK only	154 ± 4.0
No. 2	PEEK / GO(0.5)	161 ± 3.0
No. 3	PEEK / GO(1)	156 ± 2.7

Table 4.3. Flexural and compressive strength test results of the P(E2-E4)K composites.

Sample Name	Sample content (wt%)	Flexural Strength (MPa)	Compressive Strength (MPa)
No. 4	P(E2-E4)K	155 ± 3.6	125 ± 1.5
No. 5	P(E2-E4)K/CF(30)	240 ± 3.9	161 ± 2.9
No. 6	P(E2-E4)K/GO(0.5)/CF(30)	250 ± 4.0	164 ± 3.1

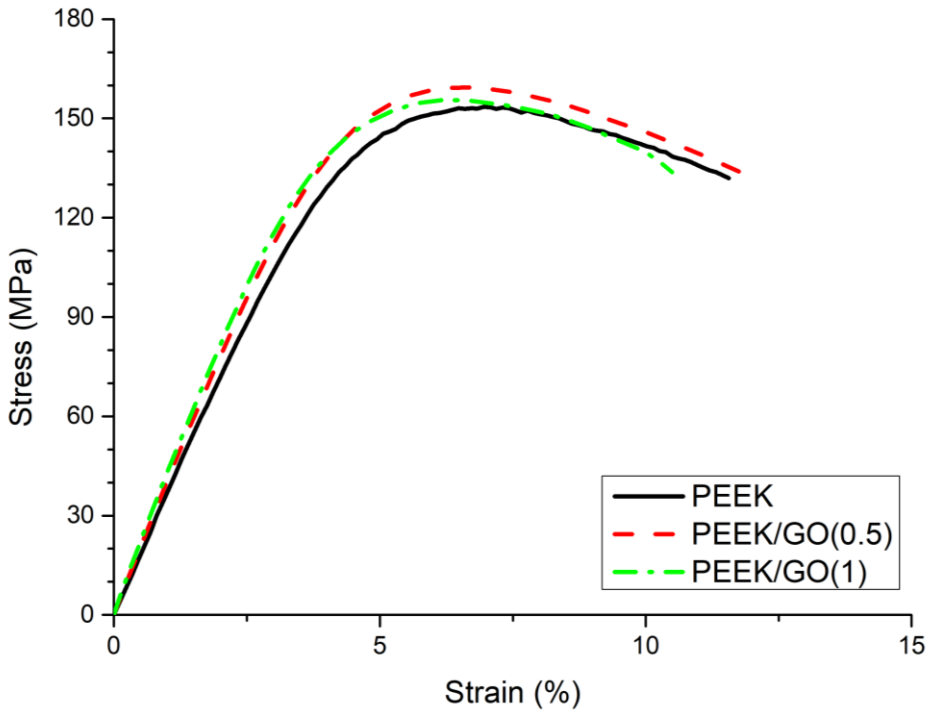

Figure 4.1. Flexural stress-strain curves of PEEK/GO composite samples.

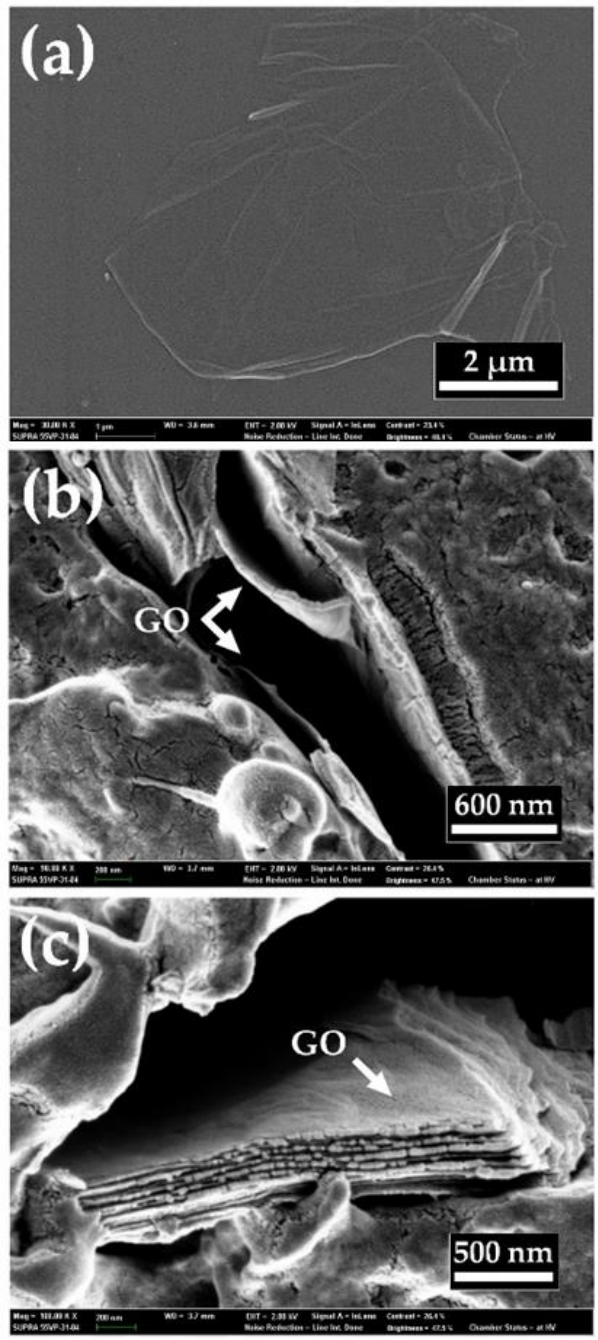

Figure 4.2. SEM images of (a) GO; and GO in the flexural fracture surface of (b) No. 2 and (c) No. 3 samples.

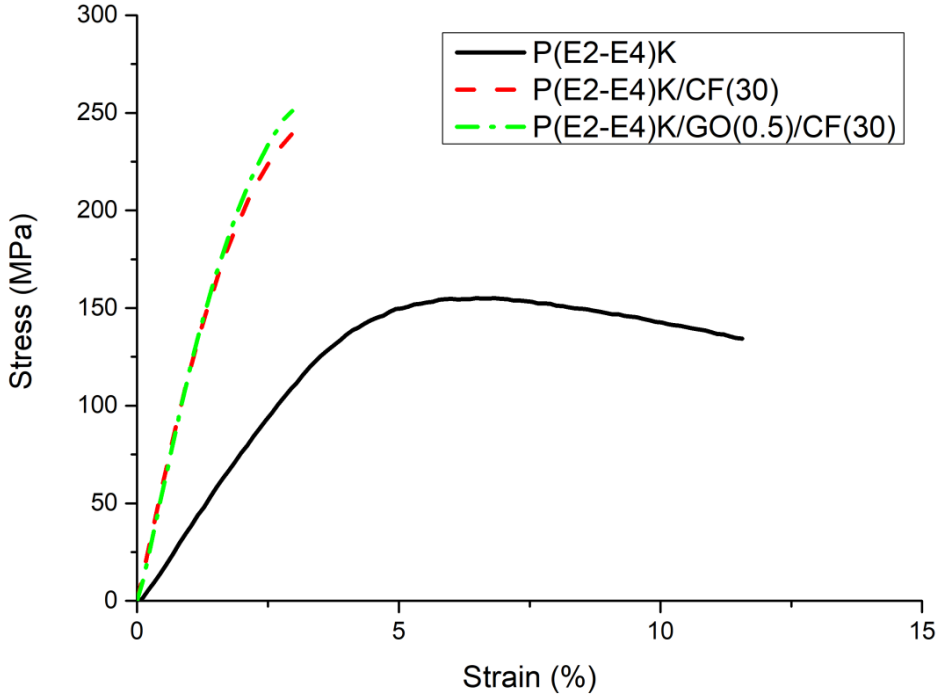

Figure 4.3. Flexural stress-strain curves of the P(E2-E4)K composite samples.

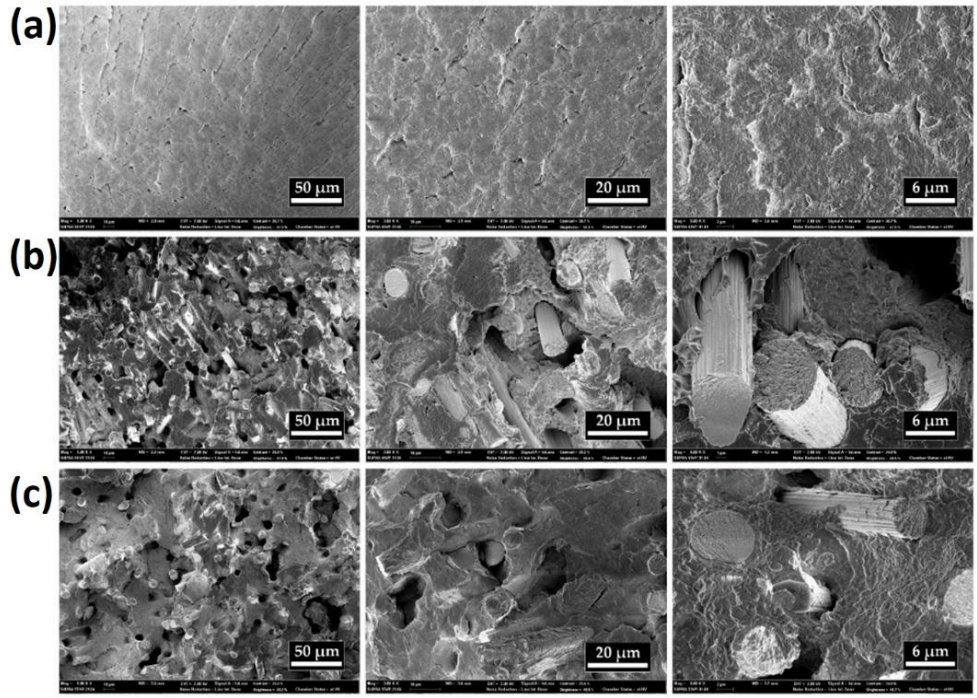

Figure 4.4. SEM images of flexural fracture surfaces of (a) No. 4, (b) No. 5, and (c) No. 6 samples.

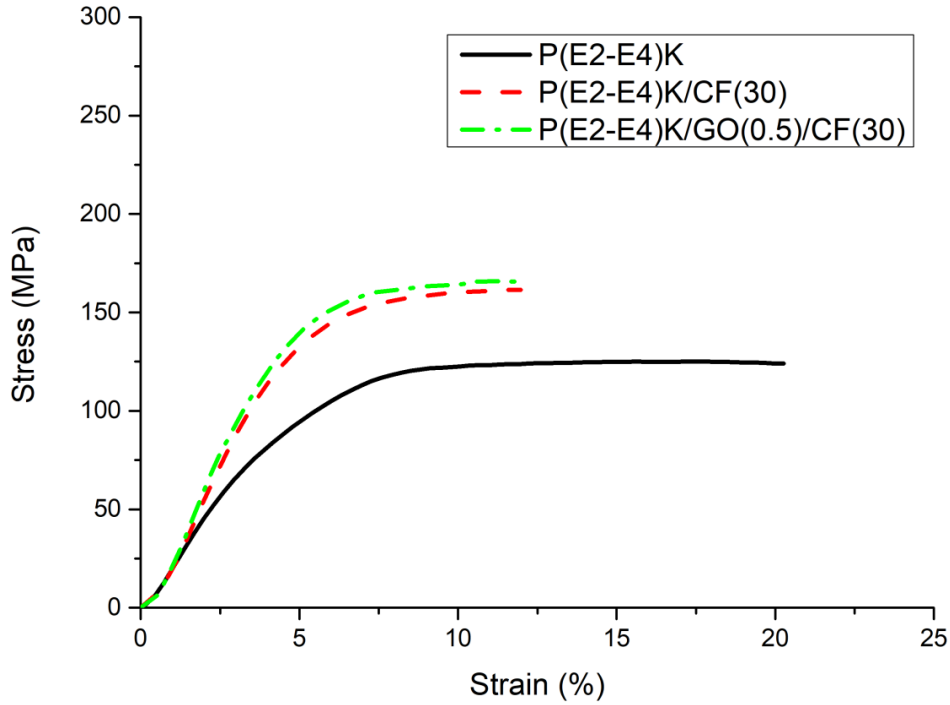

Figure 4.5. Compression stress-strain curves of the P(E2-E4)K composite samples.

4.5. References

[1] J. B. Park, R. S. Lakes, *Biomaterials: An introduction, 3rd ed*., **2007**, 100.

[2] D. J. Blackwood, *Corros. Rev*., **2003**, *21*, 97.

[3] C. K. Seal, K. Vince, M. A. Hodgson, *IOP. Conf. Ser.: Mater. Sci. Eng*., **2009**, *4*, 012011.

[4] M. Salahshoor, Y. Guo, *Materials*, **2012**, *5*, 135.

[5] S. M. Kurtz, J. N. Devine, *Biomaterials*, **2007**, *28*, 4845.

[6] C. S. James, Polym. *Composite*, **1986**, *7*, 159.

[7] B. Christian, J. W. David, E. K. Frank, J. M. William, *Polymer*, **1987**, *28*, 1009.

[8] P. C. Dawson, D. J. Blundell, *Polymer*, **1980**, *21*, 577.

[9] A. A. Mehmet-Alkan, J. N. Hay, *Polymer*, **1993**, *34*, 3529.

[10] T. E. Attwood, P. C. Dawson, J. L. Freeman, L. R. Hoy, J. B. Rose, P. A. Staniland, *Polymer*, **1981**, *22*, 1096.

[11] R. A. Clendlinning, *U.S. Pat*., **1988**, 4786694.

[12] R. A. Clendlinning, *EP. Pat*., **1987**, 0266132.

[13] J. R. Caeiro, P. González, D. Guede, *Rev. Osteoporos Metab. Miner*, **2013**, *5*, 99.

[14] P. Zioupos, J. D. Currey, *Bone*, **1998**, *22*, 57.

[15] A. Saleem, L. Frormann, A. Iqbal, *Polym. Compos*., **2007**, *28*, 785.

[16] R. Moore, P. Beredjiklian, R. Rhoad, S. Theiss, J. Cuckler, P. Ducheyne, D. G. Baker, *J. Biomed. Mater. Res*., **1997**, *34*, 137.

[17] S. R. Shin, C. Zihlmann, M. Akbari, P. Assawes, L. Cheung, K. Zhang, V. Manoharan, Y. S. Zhang, M. Yüksekkaya, K.-t Wan, M. Nikkhah, M. R. Dokmeci, X. S. Tang, A. Khademhosseini, *Small*, **2016**, *12*, 3677.

[18] W. D. Pang, Z. Ni, G. Chen, G. Huang, H. Huang, Y. Zhao, *RSC Adv*., **2015**, *5*, 63063.

[19] Y. Wang, Z. Shi, J. Fang, H. Xu, J. Yin, *Carbon*, **2011**, *49*, 1199.

[20] M. He, X. Chen, Z. Guo, X. Qiu, Y. Yang, C. Su, N. Jiang, Y. Li, D. Sun, L.

Zhang, *Compos. Sci. Technol*., **2019**, *174*, 194.

[21] K. Wang, J. Ruan, H. Song, J. Zhang, Y. Wo, S. Guo, D. Cui, *Nanoscale Res. Lett*., **2011**, *6*, 8.

[22] B. Girase, J. S. Shah, R. D. K. Misra, *Adv. Eng. Mater*., **2012**, *14*, B101.

[23] C. Chung, Y. K. Kim, D. Shin, S. R. Ryoo, B. H. Hong, D. H. Min, *Acc. Chem. Res*., **2013**, *46*, 2211.

[24] W. Pang, Z. Ni, G. Chen, G. Huang, H. Huang, Y. Zhao, *RSC Adv*., **2015**, *5*, 63063.

[25] Y. Wang, Z. Shi, J. Fang, H. Xu, J. Yin, *Carbon*, **2011**, *49*, 1199.

[26] Y. Chen, Y. Qi, Z. Tai, X. Yan, F. Zhu, Q. Xue, *Eur. Polym. J*., **2012**, *48*, 1026.

[27] P. Bhatt, A. Goel, *Mater. Sci. Res. India*, **2017**, *14*, 52.

[28] S. Peng, P. Feng, P. Wu, W. Huang, Y. Yang, W. Guo, C. Gao, C. Shuai, *Sci. Rep*., **2017**, *7*, 46604.

[29] Y. Heo, H. Im, J. Kim, *J. Membr. Sci*., **2013**, *425*, 11.

Chapter 5

Conclusion

PEEK, a semi-crystalline thermoplastic polymer, has been widely used as a spinal implant component due to its outstanding chemical resistance, biocompatibility, and mechanical properties. However, the mechanical strength and the bioactivity of PEEK should be further improved to be used as spinal implants. Thus, PEEK is mainly used as a composite reinforced with either HA or CF. Although HA has high compressive strength and excellent osteoblast proliferation ability, its severe aggregation due to a large difference in surface energy with PEEK and the ion-dipole interaction between calcium ions and hydroxyl groups on the HA surface is major problem. CFR-PEEK has been widely used in orthopedic and spinal implants because of excellent mechanical properties and corrosion resistance. However, the hydrophobicity of CF can lower the bioactivity, and the interfacial adhesion with the polymer is weak due to insufficient surface functional groups. Thus, it is important to maximize the content of HA and minimize the content of CF in the PEEK/HA/CF composite. Nevertheless, when HA and CF fillers are added at the same time, the mechanical properties and the compatibility are greatly reduced due to excessive filler use, aggregation of nano-sized HA filler, and de-bonding between the PEEK matrix and the fillers. Therefore, methods to enhance the mechanical properties of the PEEK composite by improving the dispersibility and interfacial adhesion of the fillers were studied.

First, PEEK composites were prepared by suspension blending method in ethanol. In order to enhance the dispersibility of HA nanoparticles and the interfacial adhesion between the fillers and PEEK matrix, the surface modification on the fillers with a silane coupling agent was performed. After the primary modification with APTES, the secondary modification with SAH was performed

on the fillers in order to change the surface terminal group from amine to carboxyl group, which has a negative charge and hydrophilicity. Based on the XPS and FTIR results, the surface modification of the fillers was confirmed through the formation of peaks of amide and carboxyl groups. The XRM result showed that the dispersibility of HA nanoparticles in the PEEK matrix was greatly enhanced after the surface modification. This was due to the weakened ion-dipole interaction between HA nanoparticles. After the surface modification, m-H1C3 composite showed the highest flexural modulus at 18 GPa, exceeding the flexural modulus of cortical bone. m-H1C3 sample also showed the highest flexural and compressive strength at 260 and 191 MPa, respectively. Moreover, m-H1C2 with only 20 wt% of CF filler also showed the flexural strength similar to that of cortical bone at 228 MPa. The SEM morphology showed that the surface modification on fillers not only significantly reduced the size of HA aggregates, but also improved the interfacial adhesion between the fillers and the PEEK matrix. Thus, the external stress applied to the PEEK composite could be sufficiently transferred from the polymer to the fillers. And the mechanical properties of PEEK/HA/CF composite could be improved after the surface modification.

Next, PEEK composite was prepared by introducing HA as nanofiber form. The use of HA in the form of nanofibers can improve the mechanical properties of composites with the properties of bridging, crack deflection, and pullout effects. In addition, nanofibers can expect a reduced agglomeration due to a lower surface area compared to HA nanoparticle. The XRM results confirmed that the dispersibility of nanoparticles was greatly improved when HANF was used instead of HA. When m-HANF and m-CF were used in PEEK composite, m-HF1C2

sample with 30 wt% of total filler content showed the flexural modulus similar to that of cortical bone at 13.1 GPa. Moreover, m-HF1C1, containing only 20 wt% of total filler content, showed the flexural strength similar to that of cortical bone at 209 MPa. The highest flexural strength was achieved in m-HF1C3 sample at 264 MPa. The compressive strength was also further increased by using m-HANF. The highest compressive strength was achieved in m-HF1C3 sample at 203 MPa. In short, the dispersibility of nanoparticles in PEEK composite and the interfacial adhesion between the fillers and the PEEK matrix were enhanced through the surface modification of fillers and the use of HA as nanofiber form. Furthermore, it was possible to prepare PEEK composite with mechanical properties similar to that of cortical bone even with a smaller amount of CF and a higher amount of HA.

Second, PEEK composites were prepared by mechanofusion method in dry condition to improve the dispersibility and the interfacial adhesion of fillers. The suspension blending method used in PART 2 has the advantage that it can be easily performed on a lab scale. However, this method is not convenient in industrial aspects due to solvents used and long processing time. Thereby, mechanofusion, a simple, eco-friendly, and mass productive method, seemed an adequate approach to enhance both dispersibility of aggregated filler and compatibility between polymer matrix and filler by high shear and compression forces. The SEM result showed that the HA nanoparticles were evenly dispersed and coated on the PEEK and CF surfaces after mechanofusion process. The flexural and compressive strengths of H2C2 sample prepared by mechanofusion process were increased by 26% and 13%, respectively, compared to that of H2C2 sample prepared by the suspension blending method. This was due to the enhanced dispersibility of HA and the

interfacial adhesion between the filler and the PEEK matrix. The results of XRM and SEM confirmed that the dispersion of HA aggregates was greatly improved by the mechanofusion method compared to the suspension blending method. Moreover, the interfacial adhesion between the fillers and the PEEK matrix was also improved due to the mechanical interlocking as the molten PEEK chain penetrated the microgaps between the coated HA nanoparticles and the CF surface. However, the interfacial adhesion between HA and PEEK matrix was weaker than when m-HA was used in PART2. This can be further improved by introducing a surface modification step into the fillers.

Third, the synthesized P(E2-E4)K polymer was reinforced with GO and CF fillers to prepare P(E2-E4)K/GO/CF composite. GO was expected to increase the mechanical strength of composite with a small content due to its higher surface area than CF filler. Moreover, the various surface functional groups of GO was expected to improve the interfacial adhesion with the polymer matrix and the CF filler through covalent bonding. But, the flexural strength did not significantly increase due to the aggregation of nano-sized GO. And the addition of 30 wt% of CF filler was required to match the flexural and compressive strengths of cortical bone. Thus, further research is needed to enhance the dispersibility of GO nanoparticles in P(E2-E4)K composite.

In this study, various methods such as surface modification of fillers, addition of HA as nanofiber form and mechanofusion process were applied to solve the critical issue in poor mechanical properties and dispersibility of PEEK/HA/CF composite. As a result, the mechanical properties of PEEK composite were greatly improved through enhanced dispersibility of fillers in the PEEK composite and interfacial

adhesion between fillers and PEEK matrix. Most of the existing nanofibers like cellulose nanofibers, carbon nanotubes, and collagen nanofibers have flexible properties, whereas HANF has very stiff properties. The implementation of HANF in PEEK polymer matrix suggests the possibility that the dispersibility of nanofiber can be greatly improved by using nanofibers with high stiffness due to less entanglement during the blending process. As a result, it was possible to manufacture PEEK composites having mechanical properties equivalent to that of cortical bone with 20 wt% of m-HANF content, implying higher bioactivity. However, the studies on the effect of the aspect ratio of HANF on the mechanical properties have not been reported in detail, so additional research is needed. Furthermore, the results of PEEK/HA/CF composite prepared by mechanofusion method suggested the possibility of mass production of PEEK composite with higher mechanical properties. However, the mechanical properties and the processability of PEEK composite can be further improved by using m-HANF and m-CF. In addition, the approach of using HA as nanofiber form explained in the dissertation can be universally applied to other PEEK composites that require improvements in mechanical properties. In particular, the proposed fabrication methods are expected to contribute significantly to the development of PEEK composites with high mechanical properties and bioactivity for spinal implant applications.

초 록

폴리에테르에테르케톤 (polyetheretherketone, PEEK)는 폴리아릴에테르케톤 계열의 구성원으로 케톤과 에테르 작용기를 포함하는 반 결정성 열가고성 고분자이다. PEEK는 독특한 화학 구조로 인해 뛰어난 내화학성, 기계적 특성 그리고 생체 적합성을 가지고 있다. 따라서 PEEK는 정형외과 분야에서 금속 임플란트 소재를 대체 할 수 있는 주요 후보로서 사용되어 왔다. 하지만, 척추 임플란트 소재로 사용하기에는 기계적 강도와 생체활성 특성이 부족하여 주로 탄소섬유 (carbon fiber, CF)와 수산화인회석 (hydroxyapatite, HA) 충전재가 도입되어 사용된다. 그러나 산업에서 일반적으로 쓰이는 용융 압출 공정으로 PEEK/HA/CF 복합재를 제조할 시 열악한 가공성, HA 나노 입자의 뭉침 현상, 그리고 PEEK 기지재와 충전재간의 약한 계면 결합이 문제가 된다. 그렇기에 용융 압출 공정 외에 다른 효과적인 혼합 방식과 충전재 표면 개질 도입을 통해 위의 문제들을 해결할 필요가 있다.

첫째, HA와 CF를 표면개질을 하여 현탁 혼합 (suspension blending) 방식을 통해 PEEK/HA/CF 복합재를 제조하였다. 표면개질은 실란계 커플링제 (silane coupling agent)로 1차 그리고 석신산무수물 (succinic anhydride)로 2차 개질을 진행하였다. 이렇게 제조된 PEEK/HA/CF 복합재는 기존 표면개질이 안된 충전재를 사용한 복합재에 비교하여 굴곡 및 압축 강도 모두에서 뛰어난 향상을 보였다. SEM과 XRM 분석을 활용한 형상학 분석을 통해 표면 개질된 충전재를 포함하는 복합재에서 PEEK 기지재와 충전재간의 계면접착이 크게 향상됨과 동시에 HA의 분산성이 향상 된 것을 확인하였다. 그리고 탄성률이 높은 HA 나노 섬유 (hydroxyapatite

nanofiber, HANF) 를 도입하여 복합재에 큰 물성 강화 효과를 줄 수 있었으며, 동일한 표면 개질을 통해 PEEK/HANF/CF 복합재에서 가장 뛰어난 물성 향상을 확인하였다. 이러한 향상된 물성들은 PEEK 기지재 내에서 HANF와 CF의 향상된 분산성 및 계면접착력에 의한 것이며, 이는 SEM 과 XRM 분석을 통해 확인되었다.

두 번째, 현탁 혼합 방식에는 많은 양의 용제가 쓰인다는 단점 있기에 용제가 사용되지 않는 비용융 혼합 방식인 메카노퓨전(mechanofusion) 방식으로 PEEK/HA/CF 복합재를 제조하였다. 메카노퓨전 방식을 통해 마이크로 크기인 PEEK 입자와 CF 충전재 표면에 나노 크기의 HA가 코팅이 된 것을 확인할 수 있었으며, 이는 PEEK/HA/CF 복합재 사출 성형 시 HA의 분산에 도움을 줄 수 있다. 이렇게 제조 된 복합재는 기존 현탁 혼합으로 제조된 복합재보다 더 높은 굴곡 및 압축 강도를 보였으며, XRM 분석을 통해 HA의 분산이 크게 향상되었음을 확인하였다. 또한, 표면 개질된 HA를 사용하여 메카노퓨전 방식으로 복합재를 제조하면 더 향상된 물성을 기대할 수 있다.

마지막으로, 상업용 PEEK가 아닌 합성된 P(E2-E4)K에 높은 표면적과 다양한 표면 작용기를 가지는 그래핀 옥사이드 (GO)를 도입하여 P(E2-E4)K/GO/CF 복합재를 현탁 혼합 방식으로 제조하였다. GO는 CF 대비 적은 함량으로도 높은 물성 향상을 기대하여 사용되었으나, 나노 충전재 특유의 뭉침 현상으로 인해 0.5wt% 이상 사용이 어려웠다. 하지만 CF 함량이 30wt% 포함될 시에는 척추 임플란트 소재로 쓰이기 적합한 수치의 굴곡 강도 수치를 보였다.

주요어 : 폴리에테르에테르케톤 복합재, 기계적 물성, 메카노퓨전, 현탁 혼합, 충전재 분산, 수산화인회석 나노 섬유
학 번 : 2016-21051